

1 **The varying climate feedback parameter connected to the atmosphere-ocean**  
2 **coupling and ocean circulation**

3 Diego Jiménez-de-la-Cuesta\*

4 *Max-Planck-Institut für Meteorologie, Hamburg, Deutschland*

5 \*Corresponding author: Diego Jiménez-de-la-Cuesta, diego.jimenez@mpimet.mpg.de This work  
6 has been submitted to the *Journal of Climate*. Copyright in this work may be transferred without  
7 further notice.

## ABSTRACT

8 Models indicate a time-varying radiative response of the Earth system to CO<sub>2</sub> forcing (Andrews  
9 et al. 2012; Zhou et al. 2016). This variation implies a significant uncertainty in the estimates of  
10 climate sensitivity to increasing atmospheric CO<sub>2</sub> concentration (Hawkins and Sutton 2009; Grose  
11 et al. 2018). In energy-balance models, the temporal variation is represented as an additional  
12 feedback mechanism (Winton et al. 2010; Geoffroy et al. 2013a; Rohrschneider et al. 2019), which  
13 also depends on the ocean temperature change. Models and observations also indicate that a  
14 spatio-temporal pattern in surface warming controls this additional contribution to the radiative  
15 response by modulating the tropospheric instability (Ceppi and Gregory 2017; Zhou et al. 2016).  
16 Some authors focus on the atmospheric mechanisms that drive the feedback change (Stevens et al.  
17 2016), reducing the role of the ocean's energy uptake variations. For the first time, I derive,  
18 using a linearized conceptual energy-balance model (Winton et al. 2010; Geoffroy et al. 2013a;  
19 Rohrschneider et al. 2019), an explicit mathematical expression of the radiative response and its  
20 temporal evolution. This expression connects the spatio-temporal warming pattern to a dynamical  
21 thermal capacity, stemming from changes in the ocean energy uptake. In comparison with more  
22 realistic energy-balance frameworks, and unlike the notion of additional feedback mechanisms,  
23 I show that an expanded effective thermal capacity better explains the variation of the radiative  
24 response, naturally connects with the spatio-temporal surface warming pattern and provides a  
25 non-circular framework to explain the variation of the climate feedback parameter.

26 *Significance statement.* Understanding the factors that change the Earth’s radiative response to  
27 forcing is central to reduce the uncertainty in the climate sensitivity estimates. The current  
28 atmospheric-only view on the problem of the time-varying climate feedback parameter unneces-  
29 sarily hides the ocean’s role. This work shows a novel perspective for the problem, enabling the  
30 development of a more general theory.

## 31 **1. Introduction**

32 Climate models show a wide range of temporal variation in their radiative response to CO<sub>2</sub> forcing  
33 (Senior and Mitchell 2000; Andrews et al. 2012; Ceppi and Gregory 2017). This variation appears in  
34 numerical experiments where the atmospheric CO<sub>2</sub> concentration is raised and maintained constant  
35 afterwards. The rise in the atmospheric CO<sub>2</sub> concentration modifies the Earth’s emissivity to long-  
36 wave radiation, resulting in surface warming. Surface warming modifies the radiative flux at the  
37 top of the atmosphere (TOA). The modified flux tends to cancel the energy imbalance introduced  
38 by the radiative forcing. Surface warming also changes other variables, such as the atmospheric  
39 temperature and humidity, that further modify the radiative flux. These changes are the feedback  
40 mechanisms on surface warming. The net rate at which the globally-averaged surface warming  
41 reduces the globally-averaged TOA imbalance is known as the climate feedback parameter.

42 If the feedback mechanisms did not change with time, the climate feedback parameter would be  
43 constant, and a diagram of globally-averaged TOA imbalance change  $N$  versus surface temperature  
44 change  $T_u$  ( $NT$ -diagram) would be linear. However, climate models present  $NT$ -diagrams with  
45 different degrees of curvature, indicating a non-constant climate feedback parameter (presented in  
46 Figure 1; Andrews et al. 2012; Ceppi and Gregory 2017). The degree of curvature is also modified  
47 by forcing strength (Senior and Mitchell 2000; Meraner et al. 2013; Rohrschneider et al. 2019).  
48 Temporal and state dependencies can be the root of climate feedback’s variation. Observations

49 indicate that a spatio-temporal pattern of surface warming modifies cloud feedback in decadal  
50 timescales by altering atmospheric stability, leading to feedback changes that depend not only  
51 on surface warming (Zhou et al. 2016; Mauritsen 2016; Ceppi and Gregory 2017). The spatio-  
52 temporal warming pattern should depend also on the state of the system leading to contributions  
53 to the climate feedback’s temporal and state dependencies.

54 In a globally-averaged energy-balance framework,  $N$  should be equal to the forcing  $F$  plus the  
55 radiative response of the system  $R$ ,  $N = F + R$ . Following the classical picture of the linearized  
56 feedback mechanisms depending only on the surface warming (Gregory et al. 2002)  $T_u$ , we should  
57 have  $R \sim \lambda T_u$ , where  $\lambda$  is a constant climate feedback parameter. Thus, if we consider a constant  
58 forcing  $F$ , the slope of the  $NT$ -diagram would be constant and equal to  $\lambda$ , in contradiction with  
59 observations and complex models as discussed above. Thus, either the non-linear component plays  
60 a more significant role, or the feedback mechanisms depend on more than the surface warming.

61 The problem cannot be solved by introducing more structure in the system. For instance, if  
62 we introduce two coupled layers (Winton et al. 2010; Geoffroy et al. 2013b; Rohrschneider et al.  
63 2019). One layer represents the atmosphere, land and the mixed upper ocean layer: the upper  
64 layer. The deep layer corresponds to the deep ocean. Both layers have different thermal capacities.  
65 The thermal capacities provide two timescales. One can show that these timescales only delay the  
66 equilibrium but do not alter the climate feedback parameter  $\lambda$ . For the upper layer, the energy  
67 budget is  $N_u = F + \lambda T_u - H$ , where  $H$  is the coupling between the upper and the deep layer: the  
68 deep-ocean energy uptake. The deep layer budget is, therefore,  $N_d = H$ . The sum of both budgets  
69 provides the planetary imbalance at the TOA  $N = F + \lambda T_u$ . Thus,  $N$  has the same form as before.

70 Geoffroy et al. (2013a) introduced a perturbed deep-ocean energy uptake in the upper-layer  
71 budget,  $H' := \varepsilon H$ , where  $\varepsilon$  is the efficacy parameter. The deep-layer budget is still equal to  
72  $H$ , leading to a different energy imbalance at the TOA:  $N = F + \lambda T_u + (H - H')$ . Although the

73  $H - H'$  term appears to violate the energy conservation principle, it can be interpreted as additional  
74 atmospheric feedbacks (e.g. Armour et al. 2013; Stevens et al. 2016) that depend on the deep  
75 ocean's temperature. However, this explanation seems to be ad-hoc.

76 One of the weakness of the classical approach is the linear approximation. The climate feedback  
77 parameter  $\lambda$  is defined in terms of the derivative of  $R$  evaluated at the initial state. In the same  
78 manner, the deep-ocean energy uptake  $H$  is defined in terms of a derivative evaluated at the initial  
79 state. Therefore, the seemingly ad-hoc term introduced by Geoffroy et al. (2013a) has a more  
80 concrete interpretation: the difference between the actual  $H'$  and the reference  $H$  results in a  
81 surplus  $(1 - \varepsilon)H$ . This surplus comes from a dynamically-expanded capacity of the deep ocean  
82 to uptake energy: an effective thermal capacity. This effective thermal capacity influences the  
83 flux between the upper and deep layers, modifying the surface temperature from below. Once the  
84 surface temperature is modified, the usual atmospheric feedbacks change.

85 Considering the analytical solutions of the modified two-layer model, I derive for the first time  
86 an explicit mathematical expression for the slope of the  $NT$ -diagrams, including the explicit time  
87 evolution of this slope. At its core, this expression has the ratio of change of the energy stored  
88 by the upper and deep layers and supports the more concrete interpretation that I presented above.  
89 The interpretation of these results is that the atmosphere-ocean coupling sets the spatio-temporal  
90 warming pattern. Afterwards, the atmosphere adjusts, leading to the changes in the feedback  
91 mechanisms. I first show the theory of this novel mathematical expression using the linearized  
92 two-layer model. Afterwards, I take a step back away from the approximation to show why the  
93 interpretation given above is more relevant.

## 94 2. Theory

95 The following equations define the modified linearized two-layer model (Geoffroy et al. 2013a)

$$96 \quad \begin{cases} C_u \dot{T}_u = F + \lambda T_u - \varepsilon \gamma (T_u - T_d) \\ 97 \quad C_d \dot{T}_d = \gamma (T_u - T_d) \end{cases}$$

98 where the first equation corresponds to the upper-layer budget and the second equation to the deep  
 99 layer. The parameters  $\lambda$  and  $\gamma$  are the climate feedback parameter and the rate of deep-ocean energy  
 100 uptake in the neighbourhood of the initial state.  $C_u$  and  $C_d$  are respectively the thermal capacities  
 101 (per unit area) of the upper and deep layers.  $T_u$  and  $T_d$  are temperature anomalies referred to the  
 102 initial state and the dotted quantities are time total derivatives. The planetary imbalance is the sum  
 103 of both equations, resulting in  $N = F + \lambda T_u + (1 - \varepsilon)\gamma(T_u - T_d)$ . Nonetheless, it is better to write  
 104 these equations in the following fashion

$$105 \quad \begin{cases} \dot{T}_u = F' + \lambda' T_u - \varepsilon \gamma' (T_u - T_d) \\ 106 \quad \dot{T}_d = \gamma'_d (T_u - T_d) \end{cases} \quad (1)$$

107 where  $F' := F/C_u$  with units of  $\text{K s}^{-1}$  and,  $\lambda' := \lambda/C_u$ ,  $\gamma' := \gamma/C_u$  and  $\gamma'_d := \gamma/C_d$  with units  
 108 of  $\text{s}^{-1}$ . Equations (1) are a system of linear ordinary differential equations (Geoffroy et al.  
 109 2013a; Rohrschneider et al. 2019). Although the solutions are standard and widely discussed in  
 110 other articles (e.g. Geoffroy et al. 2013a; Rohrschneider et al. 2019), here I will use the normal  
 111 mode approach. In the following, I proceed by summarizing the relevant facts, leaving the full  
 112 mathematical discussion to the appendix A of this article.

113 The homogeneous ( $F' \equiv 0$ ) version of the system (1) has two distinct eigenvalues  $\mu_{\pm} := (\hat{\lambda} \pm \kappa)/2$ ,  
 114 where  $\hat{\lambda} := \lambda' - \varepsilon \gamma' - \gamma'_d$  and  $\kappa^2 := \hat{\lambda}^2 + 4\lambda' \gamma'_d$ . These eigenvalues provide two distinct eigenvectors,  
 115 forming a basis in which the full system (1) is uncoupled and, therefore, has a straight-forward  
 116 solution. The eigensolutions  $T_{\pm}$  are the solutions associated with each eigenvalue. Afterwards,  
 117 one can return to the original representation, finding that  $T_u$  and  $T_d$  are linear combinations of

118  $T_{\pm}$ . These linear combinations are the normal modes: the symmetric mode  $T_s := T_+ + T_-$  and the  
 119 antisymmetric mode  $T_a := T_+ - T_-$ . The main result of this process is that  $T_u = T_s$  and  $T_d = \alpha T_s + \beta T_a$ ,  
 120 where  $\alpha$  and  $\beta$  are scalars that depend on the coefficients of the system (1). The normal-mode  
 121 representation makes explicit the coupling of the deep layer with the upper layer.

### 122 3. Results

123 (i) *The explicit slope of the NT–diagram* From the solutions to system (1) written in terms of the  
 124 normal modes, one can obtain an expression for the slope of the NT–diagram,  $\dot{N}/\dot{T}_u$ , of a system  
 125 under constant forcing. In the appendix, I derive the following closed expression for the slope  
 126 in terms of the derivatives of the normal modes and as a factor of the constant climate feedback  
 127 parameter  $\lambda$

$$128 \quad \frac{\dot{N}}{\dot{T}_u} = \left\{ \frac{\varepsilon + 1}{2\varepsilon} + \frac{\varepsilon - 1}{2\varepsilon} \frac{C_u \kappa}{|\lambda|} \left[ \left( \frac{\varepsilon}{C_u} + \frac{1}{C_d} \right) \frac{\gamma}{\kappa} - \frac{\dot{T}_a}{\dot{T}_s} \right] \right\} \lambda \quad (2)$$

130 The main characteristic of equation (2) is the square-bracket term of its right-hand side. It contains  
 131 two parts. The first one sets a basic enhanced slope and contains the sum of the inverse of the  
 132 thermal capacities as if we had an electrical circuit with capacitors in series. The second part  
 133 provides the time evolution. It is a ratio of the changes in energy content. This ratio compares the  
 134 change in energy content of the deep layer with that of the upper layer. To confirm the importance  
 135 of the square-bracket term, one can take the limit as  $\varepsilon \rightarrow 1$ , where the pattern effect is cancelled in  
 136 equation (2)

$$137 \quad \lim_{\varepsilon \rightarrow 1} \frac{\dot{N}}{\dot{T}_u} = \lambda$$

138  
 139 The strong coupling between the upper and deep layers disappears. We end up with a constant  
 140 slope. However, if  $\varepsilon \neq 1$ , the climate feedback parameter varies with the ratio of the changes in

141 energy content from the deep to the upper layer around a basic value that depends on the thermal  
 142 capacities of the system, the square bracket term in equation (2).

143 (ii) *Explicit expression for the ratio term* Using the full mathematical expressions for the solutions  
 144  $T_s$  and  $T_a$  for constant forcing, I write the ratio term in equation (2) as

$$145 \quad \frac{\dot{T}_a}{\dot{T}_s} = \tanh \left[ \frac{\kappa}{2}(t - t_0) + \operatorname{arctanh} \left( \frac{\hat{\lambda} + 2\gamma'_d}{\kappa} \right) \right] \quad (3)$$

147 The ratio (3) grows in a sigmoidal fashion from  $-1$  to  $1$ . This hyperbolic tangent has a scaling  
 148 factor  $(\kappa/2)$  that sets the rate of change of the hyperbolic tangent between its extreme values. It also  
 149 has a shift (the  $\operatorname{arctanh}$  term) that determines when the hyperbolic tangent crosses zero, governing  
 150 the contribution of the last term in equation (2). Both scaling and shift are in terms of  $C_u$ ,  $C_d$ ,  $\varepsilon$ ,  $\gamma$   
 151 and  $\lambda$ .

152 The interpretation of equation (3) is that, after the initial forcing, the deep ocean warms up slower  
 153 than the upper layer, steepening the slope of the  $NT$ -diagram. Once the ratio reaches the sign-  
 154 reversal point, the last term's contribution in equation (2) only flattens the slope of the  $NT$ -diagram.  
 155 The scaling factor and the shift of the ratio (3) set the timescale for the flattening. Equation (3)  
 156 expresses precisely the time evolution of the climate feedback parameter that others have only  
 157 approximated through numerical experiments with the modified two-layer model (Geoffroy et al.  
 158 2013a; Rohrschneider et al. 2019). Additionally, it establishes a third timescale in the Earth system,  
 159 related to the atmosphere-ocean coupling.

160 (iii) *Explicit expression of the climate feedback parameter* Using the explicit expressions, the  
 161 equation (2) for the climate feedback parameter is

$$162 \quad \frac{\dot{N}}{\dot{T}_u} = \frac{\varepsilon + 1}{2\varepsilon} \left( 1 + \frac{\varepsilon - 1}{\varepsilon + 1} \frac{C_u \kappa}{|\lambda|} \left[ \left( \frac{\varepsilon}{C_u} + \frac{1}{C_d} \right) \frac{\gamma}{\kappa} - \tanh \left( \frac{\kappa}{2}(t - t_0) + \operatorname{arctanh} \left( \frac{\hat{\lambda} + 2\gamma'_d}{\kappa} \right) \right) \right] \right) \lambda \quad (4)$$

164 The factor of  $\lambda$  is composed of terms that are positive except for the ratio term coming from  
 165 equation (3). One can prove that at the start ( $t = t_0$ ) the slope is

$$166 \quad \frac{\dot{N}}{\dot{T}_u}(t_0) = \left(1 + (\varepsilon - 1) \frac{\gamma}{|\lambda|}\right) \lambda$$

168 and from here up to the sign reversal of the ratio term, the slope flattens. The flattening is gentle  
 169 at first, but towards the sign reversal it accelerates.

170 At the time of sign reversal we have

$$171 \quad \frac{\dot{N}}{\dot{T}_u}(t_{\text{rev}}) = \frac{\varepsilon + 1}{2\varepsilon} \left(1 + \frac{\varepsilon - 1}{\varepsilon + 1} \left(\frac{\varepsilon}{C_u} + \frac{1}{C_d}\right) \frac{C_u \gamma}{|\lambda|}\right) \lambda$$

173 and from here and on, the ratio term becomes positive, leading to an even flatter slope. The flattening  
 174 decelerates and becomes gentle again. The asymptotic value of the slope of the  $NT$ -diagram is

$$175 \quad \lim_{t \rightarrow \infty} \frac{\dot{N}}{\dot{T}_u} = \frac{\varepsilon + 1}{2\varepsilon} \left(1 + \frac{\varepsilon - 1}{\varepsilon + 1} \frac{C_u \kappa}{|\lambda|} \left[\left(\frac{\varepsilon}{C_u} + \frac{1}{C_d}\right) \frac{\gamma}{\kappa} - 1\right]\right) \lambda$$

177 *(iv) Numerical estimates of the atmosphere-ocean coupling* By substituting in expression (4) the  
 178 parameter values found by Geoffroy et al. (2013a), I find the timescale for the sign reversal of the  
 179  $\dot{T}_a/\dot{T}_s$  ratio term. I use the multimodel mean values reported by Geoffroy et al. (2013a). For the  
 180 multimodel average values ( $C_u = 8.2 \text{ W yr m}^{-2} \text{ K}^{-1}$ ,  $C_d = 109 \text{ W yr m}^{-2} \text{ K}^{-1}$ ,  $\gamma = 0.67 \text{ W m}^{-2} \text{ K}^{-1}$ ,  
 181  $\lambda = -1.18 \text{ W m}^{-2} \text{ K}^{-1}$  and  $\varepsilon = 1.28$ ) the sign reversal of the ratio term takes place after 18.3 years.  
 182 This timescale lies between the fast (4.2 years) and slow (290 years) timescales established in terms  
 183 of the thermal capacities alone (Geoffroy et al. 2013a). This timescale is when we are at one half  
 184 of the change between the initial and final values of the slope.

185 I calculate the time for sign reversal using the rest of values in the tables of Geoffroy et al. (2013a)  
 186 and obtain that the multimodel average is 18.8 years. The minimum value is 8.8 years for GISS-  
 187 E2-R, whereas the maximum is 25.1 years for CNRM-CM5.1. If I compare with their estimates  
 188 of the fast and the slow timescales, even the extreme values fit well between both. Enlightening is

189 that the timescale of the sign reversal seems to fit with the de-facto 20-year standard to evaluate  
190 the change in slope (e.g. Ceppi and Gregory 2017).

191 I also compare between the multimodel averages for all parameters and with the thermal ca-  
192 pacities as calculated by Jiménez-de-la-Cuesta and Mauritsen (2019):  $C_u = 7.2 \text{ W yr m}^{-2} \text{ K}^{-1}$ ,  
193  $C_d = 367 \text{ W yr m}^{-2} \text{ K}^{-1}$ . The calculated deep-layer thermal capacity is larger than the CMIP5  
194 multi-model average, whereas the calculated value for the upper layer is smaller than the CMIP5  
195 average. From these differences, we can note changes in the slope evolution (figure 2). Although  
196 the difference in final slopes is small, the calculated thermal capacities strongly shift the sign-  
197 reversal timescale: a deeper deep ocean lengthens the sign-reversal timescale, whereas a shallower  
198 upper layer shortens it.

#### 199 **4. Analysis and Discussion**

200 *(i) Consequences of the equation (4)* We have two terms in the factor of equation (4): the identity  
201 term and the  $(\varepsilon - 1)$ -term. The second term is only active if  $\varepsilon \neq 1$ , and has two contributions.  
202 The first one is a constant contribution linked to the thermal capacities of the system. The second  
203 contribution is time-varying and depends on the ratio  $\dot{T}_a/\dot{T}_s$ . This ratio measures the proportion of  
204 energy that goes into the deep ocean compared to that stored in the upper layer. Together, these  
205 terms provide a physical picture in which the slope's variation is determined by a basic thermal  
206 capacity, which is expanded dynamically. The expansion stems from the changing energy fluxes  
207 between the upper and deep layers that differ from the flux at the starting state represented by  $\gamma$ . This  
208 flux difference changes the surface temperature and connects with the evolving spatio-temporal  
209 warming pattern in a more concrete fashion, given that the evolution and spatial distribution of the  
210 sea surface temperature corresponds to changes in the energy fluxes.

211 I showed above that the thermal capacities have a strong effect on the timescale at which the slope  
212 of the  $NT$ -diagram changes (figure 2). Thermal capacities in complex models depend strongly on  
213 the depth of the ocean mixed-layer and, therefore, on the atmosphere-ocean coupling, providing  
214 diverse behaviors (figure 3)

215 The above interpretation of the two-layer model in the context of the real Earth System is the  
216 following: The relative change in the energy fluxes due to the atmosphere-ocean coupling com-  
217 pels the atmospheric feedbacks to adjust. Thus, the magnitude of the changes in the atmospheric  
218 radiative response depend on the atmosphere-ocean coupling. One can argue that the non-local  
219 free-tropospheric warming from the deep-convective warm regions is enough to explain the change  
220 in feedbacks. However, for the pattern effect to act as proposed by Zhou et al. (2016); Mauritsen  
221 (2016); Ceppi and Gregory (2017), one needs the surface temperature variation in the subsidence  
222 areas. Here the atmosphere-ocean coupling and oceanic circulation enter to change the surface tem-  
223 perature, determining the spatio-temporal warming pattern. Thus, the atmosphere-ocean coupling  
224 can play a larger role than thought before (Kiehl 2007).

225 *(ii) State and forcing dependence* In this article, I ignored the dependence on the strength of  
226 forcing (Senior and Mitchell 2000; Meraner et al. 2013; Rohrschneider et al. 2019). However, such  
227 dependence should come from the reference values  $\varepsilon$ ,  $\lambda$  and  $\gamma$  that exist under a particular forcing.  
228 Values of  $\lambda$  and  $\gamma$  are first-order derivatives in the neighbourhood of the starting states. Therefore,  
229 we need to explore the physics behind the  $\varepsilon$  parameter to understand how it can change depending  
230 on forcing. The physics of  $\varepsilon$  is the atmosphere-ocean coupling, including circulation. Therefore,  
231 we should explore how forcing impacts the atmosphere-ocean coupling, resulting in changes in the  
232 spatio-temporal warming pattern.

233 There are versions of linearized energy balance models in which a simple non-linear term is  
 234 introduced (Rohrschneider et al. 2019). Although higher-order terms in the Taylor expansion of  
 235 either the radiative response  $R$  or the energy uptake  $H$  can provide additional information, the  
 236 dependencies arising from the atmosphere-ocean coupling, as shown in this article, are far more  
 237 important in light of the results presented above.

238 *(iii) Non-linear planetary energy balance* Above I presented evidence favouring the ocean's  
 239 energy uptake central role in determining the spatio-temporal warming pattern and its effects on  
 240 the atmospheric feedback mechanisms. I test this idea in a more general theoretical framework by  
 241 writing the planetary energy budget in another widely-known representation

$$242 \quad \frac{d}{dt}(CT_u) = (1 - \alpha)S + G - \epsilon\sigma(fT_u)^4 \quad (5)$$

244 where  $S := S(t)$  in  $\text{W m}^{-2}$  is the incoming solar radiative flux at the TOA,  $\alpha$  is the planetary  
 245 albedo,  $G := G(t)$  in  $\text{W m}^{-2}$  represents the remaining inputs (natural and anthropogenic), and  
 246 the last term is the usual planetary long-wave emission, in  $\text{W m}^{-2}$ , as a grey-body of emissivity  
 247  $\epsilon$  and surface temperature  $T_u$  with  $f$  the lapse-rate scaling factor for the emission temperature.  
 248 At first inspection, we have the origin of the feedback mechanisms: the planetary albedo  $\alpha$ , the  
 249 emissivity  $\epsilon$  and the scaling factor  $f$ . On the one hand, we have the short-wave strand, the planetary  
 250 albedo  $\alpha := \alpha(T_u, q_{cld,w}, \dots)$  that is a function of, e.g., the surface temperature (determining ice-  
 251 sheet and sea-ice area) and the amount of liquid water in the atmosphere forming clouds. On  
 252 the other hand, we have the long-wave thread, the emissivity and the lapse-rate scaling factor  
 253  $\epsilon, f := f(T_u, q_v, q_{cld,w}, \dots)$ , depending on, e.g. the surface temperature, and the amount of water  
 254 vapor and cloud liquid water in the atmosphere.

255 The atmospheric feedback mechanisms cannot rely on any temperature we define inside the  
 256 ocean. The ocean affects  $\alpha$ ,  $\epsilon$  and  $f$  only through changing  $T_u$ . In equation (5), we cannot see such

257 dependence. Therefore, here we would be tempted to artificially introduce it by saying that  $\alpha$ ,  $\epsilon$   
 258 and  $f$  depend on another temperature in the ocean, as others have interpreted from the modified  
 259 two-layer model. In this work, I have shown that there is another more natural place where the  
 260 ocean enters into play: the energy imbalance at the TOA,  $N$ .

261 We usually picture  $N$  as  $N = (d/dt)(CT_u) = C\dot{T}_u$ . However, we can have processes that modify the  
 262 thermal capacity: For example, (a) if the mixed-layer depth varies, it modifies the amount of water  
 263 in contact with the atmosphere; (b) deep-water upwelling not only reduces the surface temperature  
 264 but increases the thermal capacity of the mixed layer; (c) a similar effect comes from water from  
 265 ice sheet melting. Therefore, the sea surface temperature is controlled by the oceanic circulation  
 266 and the ocean-atmosphere interaction, setting the warming pattern. Thus, a more proper definition  
 267 for  $N$  is  $N = (d/dt)(CT_u) - \dot{C}T_u = C\dot{T}_u$ . The term  $\dot{C}T_u$  considers these processes that modify the sea  
 268 surface temperature and the ocean energy fluxes from below.

269 If we rewrite equation (5) using the corrected  $N$ :

$$270 \quad N = (1 - \alpha)S + G - \epsilon\sigma(fT_u)^4 - \dot{C}T_u \quad (6)$$

271

272 The last term of equation (6) is the representation of the effect of the spatio-temporal warming  
 273 pattern. The factor  $\dot{C}$  needs a new differential equation that describes the temporal variations of  
 274 the energy uptake due to the ocean circulation and atmosphere-ocean interactions. If we want to  
 275 use this non-linear framework, we would also need additional differential equations or constitutive  
 276 relationships for  $\alpha$ ,  $\epsilon$  and  $f$ .

277 However, to look at the effect of this additional dynamical thermal capacity term on the atmo-  
 278 spheric feedbacks, let us consider the total derivative of  $N$ . In the appendix B, I present the details

279 of this derivation. The expression for the total derivative of equation (6) divided by  $\dot{T}_u$  is

$$\begin{aligned}
 \frac{\dot{N}}{\dot{T}_u} &= \left[ (1 - \alpha) \frac{\dot{S}}{\dot{T}_u} + \frac{\dot{G}}{\dot{T}_u} \right] \\
 &- \left[ 1 + \frac{S}{4\epsilon\sigma f(fT_u)^3} \frac{\dot{\alpha}}{\dot{T}_u} + \frac{T_u}{4\epsilon} \frac{\dot{\epsilon}}{\dot{T}_u} + \frac{T_u}{f} \frac{\dot{f}}{\dot{T}_u} + \frac{\dot{C}}{4\epsilon\sigma f(fT_u)^3} + \frac{T}{4\epsilon\sigma f(fT_u)^3} \frac{\dot{C}}{\dot{T}_u} \right] 4\epsilon\sigma f(fT_u)^3 \quad (7)
 \end{aligned}$$

283 The first term is the contribution from the forcing variation, whereas the second term is the  
 284 contribution of the radiative response. This last term is the analogue for the expression of the  
 285 square bracket term in equation (2). This last term has a non-dimensional factor multiplying  
 286 the product of Planck feedback. In the non-dimensional factor we have a sum of terms. Each  
 287 term represents the contributions of feedbacks and other processes to the radiative response in  
 288 comparison to the Planck feedback. The first term in this factor is one, for the Planck feedback.  
 289 The second term is the contribution of the planetary-albedo feedback, including surface albedo as  
 290 well as short-wave cloud feedback. The third term is the contribution of the emissivity feedback,  
 291 including water-vapor feedback. The fourth term is the lapse-rate feedback. The last two terms  
 292 are the contribution of the atmosphere-ocean interaction and ocean circulation to the radiative  
 293 response.

294 Equation (7) is the non-linear analogue of equation (2) if we consider that the forcing is stationary.  
 295 In a linearization, the first four terms would provide a term analogous to  $\lambda$ . The last two terms,  
 296 considering that at least  $\dot{C} \neq 0$ , would provide the analogue of the remaining terms corresponding  
 297 to a situation where  $\varepsilon \neq 1$ . If  $\varepsilon = 1$ , then  $\dot{C} = 0$  and the linearization of equation (7), would  
 298 provide a constant feedback parameter if we accept that  $\alpha$ ,  $\epsilon$  and  $f$  covary with  $T_u$  except for sign.  
 299 These facts provide more support for interpreting the modified two-layer model as introducing  
 300 a dynamical thermal capacity, turning the limelight to the role of the ocean circulation and the  
 301 atmosphere-ocean interactions in setting the sea surface temperature patterns.

## 302 5. Conclusions

303 I presented for the first time an explicit mathematical expression of the slope of the  $NT$ -diagrams.  
304 For that end, I used the linearized framework of the two-layer energy balance model. From the  
305 analysis, I uncover another timescale in the Earth System: the timescale of the changes of the  
306 climate feedback parameter. The timescale is related to the ratio of change in the energy content  
307 between the deep- and the upper-layer (atmosphere, land and mixed upper ocean). In CMIP5  
308 models this time scale is around 18 years, providing theoretical support to the 20-year standard  
309 timescale used to study the change in the climate feedback parameter.

310 The mathematical expression and the analysis of the modified linearized two-layer model suggest  
311 that the spatio-temporal warming pattern is a product of the atmosphere-ocean coupling (the  $H$  term  
312 in equations). Linearization uses the value of the coupling at the starting state. When introducing  
313 a modified coupling ( $H'$ ) that represents departures from the starting state, the modified two-layer  
314 model can represent the variation of the slope of the  $NT$ -diagrams. The found mathematical  
315 expression suggest that the difference  $H - H'$  acts as a dynamically-enlarged thermal capacity  
316 that depends on the ratio of change in the energy content between layers, changing the surface  
317 temperature. In the real Earth System, therefore, the atmosphere-ocean coupling and the circula-  
318 tion produce the evolving spatio-temporal warming pattern, to which the atmospheric feedbacks  
319 respond. I also shortly discussed this interpretation in terms of a non-linear framework, where  
320 feedback mechanisms not depending on the surface temperature are complicated to introduce. In-  
321 stead of introducing exogenous dependencies in the feedback terms, the solution is that the thermal  
322 capacity of the system varies. The variation represents the atmosphere-ocean coupling and ocean  
323 circulation and relates to the spatio-temporal surface warming pattern. Its effect on the surface  
324 temperature then seamlessly translates to changes on the atmospheric feedback mechanisms.

325 *Acknowledgments.* I thank Hauke Schmidt, Jiawei Bao, Christopher Hedemann and Moritz Gün-  
326 ther for reading and correcting the manuscript and for the lively discussions on how to present this  
327 highly theoretical ideas.

328 *Data availability statement.* All the data used by this study is described fully in the main text.  
329 The numbers for reproducing the figure 2 and 3 are contained in the articles by Geoffroy et al.  
330 (2013a) and Jiménez-de-la-Cuesta and Mauritsen (2019). The theoretical considerations are fully  
331 described in the appendix to this article. Therefore, this article is fully reproducible and almost  
332 self contained.

## 333 APPENDIX A

### 334 **Mathematical analysis of the modified two-layer model**

335 In Classical Mechanics, a very coarse thinking would be reducing the field to the task of solving  
336 the equation  $\dot{\mathbf{p}} = \mathbf{F}$  for any force term, either analytically or numerically. Going further leads to  
337 conservation principles and formulations of Classical Mechanics that provide more information  
338 without actually obtaining solutions, if that is possible at all. In this appendix, reduced to the scale  
339 of a simplified framework, I show that by delving deep into the mathematics of a system of linear  
340 ordinary differential equations, the structure of the solutions and its physical interpretation, one  
341 can obtain a new view on an old problem.

342 The appendix is written in an exhaustive way and I leave few things without development. The  
343 cases in which I do not show some algebraic step is because the necessary step has been already  
344 done or is very simple.

## 345 **Matrix form of the equations**

346 The equations of two-layer model Geoffroy et al. (2013a) are

$$\begin{aligned}
 347 \quad N_u &= C_u \dot{T}_u = F + \lambda T_u - \varepsilon \gamma (T_u - T_d) \\
 348 \quad N_d &= C_d \dot{T}_d = \gamma (T_u - T_d)
 \end{aligned} \tag{A1}$$

349 and the planetary imbalance is  $N = N_u + N_d$ . I present another form of the equations, where I divide  
 350 by the thermal capacities.

$$\begin{aligned}
 351 \quad \dot{T}_u &= \frac{F}{C_u} + \frac{\lambda}{C_u} T_u - \varepsilon \frac{\gamma}{C_u} (T_u - T_d) \\
 352 \quad \dot{T}_d &= \frac{\gamma}{C_d} (T_u - T_d)
 \end{aligned}$$

353 If I define  $F' := F/C_u$ ,  $\lambda' := \lambda/C_u$ ,  $\gamma' := \gamma/C_u$ ,  $\gamma'_d := \gamma/C_d$ , one can write the equations in a lean  
 354 way

$$\begin{aligned}
 355 \quad \dot{T}_u &= F' + \lambda' T_u - \varepsilon \gamma' (T_u - T_d) \\
 356 \quad \dot{T}_d &= \gamma'_d (T_u - T_d)
 \end{aligned} \tag{A2}$$

357 I will put the system in matrix form. I define  $\mathbf{T} := (T_u, T_d)$ ,  $\mathbf{F}' := (F', 0)$  and

$$358 \quad \mathbf{A} := \begin{pmatrix} \lambda' - \varepsilon \gamma' & \gamma'_d \\ \varepsilon \gamma' & -\gamma'_d \end{pmatrix} \tag{A3}$$

360 and the system can be written

$$361 \quad \dot{\mathbf{T}} = \mathbf{F}' + \mathbf{TA} \tag{A4}$$

363 which is the representation of the system in the temperature basis.

## 364 **Eigenvalues and eigenvectors**

365 I want to analyse the normal modes of the system. For that end, I need the eigenvalues of the  
 366 homogeneous system obtained as the solutions of the characteristic equation

$$367 \quad (\lambda' - \varepsilon \gamma' - \mu)(-\gamma'_d - \mu) - \varepsilon \gamma' \gamma'_d = 0 \tag{A5}$$

369

370

$$-\lambda' \gamma'_d + \varepsilon \gamma' \gamma'_d + \mu \gamma'_d - \lambda' \mu + \varepsilon \gamma' \mu + \mu^2 - \varepsilon \gamma' \gamma'_d = 0$$

371

$$-\lambda' \gamma'_d + \mu \gamma'_d - \lambda' \mu + \varepsilon \gamma' \mu + \mu^2 = 0$$

372

373

$$-\lambda' \gamma'_d - (\lambda' - \varepsilon \gamma' - \gamma'_d) \mu + \mu^2 = 0$$

374 The solutions of equation (A5) are

375

376

$$\mu = \frac{(\lambda' - \varepsilon \gamma' - \gamma'_d) \pm [(\lambda' - \varepsilon \gamma' - \gamma'_d)^2 + 4\lambda' \gamma'_d]^{1/2}}{2} \quad (\text{A6})$$

377

378

379

and, given that in the Earth  $C_u < C_d$ , one can prove that there are two real and different eigenvalues. One needs to check that the square root term is not complex or zero. This only happens if the sum within the square root is negative or zero

380

$$(\lambda' - \varepsilon \gamma' - \gamma'_d)^2 + 4\lambda' \gamma'_d \leq 0$$

381

$$(\lambda' - \varepsilon \gamma')^2 - 2(\lambda' - \varepsilon \gamma') \gamma'_d + \gamma'_d{}^2 + 4\lambda' \gamma'_d \leq 0$$

382

$$\lambda'^2 - 2\lambda' \varepsilon \gamma' + (\varepsilon \gamma')^2 - 2(\lambda' - \varepsilon \gamma') \gamma'_d + \gamma'_d{}^2 + 4\lambda' \gamma'_d \leq 0$$

383

$$\lambda'^2 - 2\lambda' \varepsilon \gamma' + (\varepsilon \gamma')^2 - 2\lambda' \gamma'_d + 2\varepsilon \gamma' \gamma'_d + \gamma'_d{}^2 + 4\lambda' \gamma'_d \leq 0$$

384

$$(\lambda' / \gamma'_d)^2 - 2(\lambda' / \gamma'_d) \varepsilon (\gamma' / \gamma'_d) + (\varepsilon (\gamma' / \gamma'_d))^2 + 2\varepsilon (\gamma' / \gamma'_d) + 1 + 2(\lambda' / \gamma'_d) \leq 0$$

385

$$(\lambda' / \gamma'_d)^2 - 2(\lambda' / \gamma'_d) [\varepsilon (\gamma' / \gamma'_d) - 1] + (\varepsilon (\gamma' / \gamma'_d))^2 + 2\varepsilon (\gamma' / \gamma'_d) + 1 \leq 0$$

386

$$(\lambda' / \gamma'_d)^2 - 2(\lambda' / \gamma'_d) [\varepsilon (\gamma' / \gamma'_d) - 1] + (\varepsilon (\gamma' / \gamma'_d) + 1)^2 \leq 0$$

387

388

$$(\lambda' / \gamma'_d)^2 + (\varepsilon (C_d / C_u) + 1)^2 \leq 2(\lambda' / \gamma'_d) [\varepsilon (C_d / C_u) - 1]$$

389

390

391

392

In the last inequality, the left-hand side is always positive. The right-hand side depends on the sign of the factors. The middle factor is negative since  $\lambda'$  is negative and  $\gamma'_d$  is positive. The third factor is positive provided that  $\varepsilon > C_u / C_d$ . Given that  $\varepsilon \geq 1$  and  $C_u < C_d$ , then the third factor is positive in our case. Then the right-hand side is negative. Thus, we obtained a contradiction

393 by supposing that the square root term was negative or zero. Therefore, the conclusion is that  
 394 the eigenvalues are two real and distinct numbers. Some CMIP5 models show  $\varepsilon < 1$  according  
 395 to Geoffroy et al. (2013a). These also fit here. In the last condition of the above expression we  
 396 require that  $\varepsilon(C_d/C_u) - 1 > 0$ . If  $\varepsilon \geq C_u/C_d$  this is fulfilled.  $C_u/C_d$  is a small quantity and, in the  
 397 models that have a lesser than one  $\varepsilon$ , always the  $\varepsilon$  is larger than this small quantity by an order of  
 398 magnitude. Thus, what I had said until now and will be said afterwards applies to all cases.

399 I call the solutions  $\mu_+$  and  $\mu_-$ , depending on the sign of the square root term. Let us rewrite their  
 400 expression in more lean fashion. I define  $\hat{\lambda} := \lambda' - \varepsilon\gamma' - \gamma'_d$  and we call  $\kappa$  the square root term.  
 401 Then, I rewrite the solutions (A6) as

$$402 \mu_{\pm} = \frac{\hat{\lambda} \pm \kappa}{2} \quad (A7)$$

404 Now that I know the eigenvalues, one should get the eigenvectors of the system and solve it  
 405 easily. The eigenvectors are the generators of the kernel of the operators  $\mathbf{A} - \mu_{\pm} \text{id}$ . Let us write  
 406 the diagonal of the matrix  $\mathbf{A}$  with the definition of  $\hat{\lambda}$

$$407 \mathbf{A} = \begin{pmatrix} \hat{\lambda} + \gamma'_d & \gamma'_d \\ \varepsilon\gamma' & \hat{\lambda} - (\lambda' - \varepsilon\gamma') \end{pmatrix}$$

409 and then the matrices for each eigenvalue have the form

$$410 \mathbf{A} - \mu_{\pm} \text{id} = \begin{pmatrix} \hat{\lambda} + \gamma'_d - \mu_{\pm} & \gamma'_d \\ \varepsilon\gamma' & \hat{\lambda} - (\lambda' - \varepsilon\gamma') - \mu_{\pm} \end{pmatrix}$$

$$411 = \begin{pmatrix} \mu_{\mp} + \gamma'_d & \gamma'_d \\ \varepsilon\gamma' & \mu_{\mp} - (\lambda' - \varepsilon\gamma') \end{pmatrix}$$

413 Since eigenvalues are real and distinct, there should be two linearly-independent eigenvectors,  
 414 one for each eigenvalue. These vectors should fulfill that  $\mathbf{e}_{\pm}(\mathbf{A} - \mu_{\pm} \text{id}) = 0$ . Solving that linear

415 system, I find the eigenvectors in temperature representation

$$416 \quad \mathbf{e}_{\pm} = \mathbf{e}_u - \frac{\mu_{\mp} + \gamma'_d}{\varepsilon\gamma'} \mathbf{e}_d \quad (A8)$$

417

418 The procedure to get the result is to solve the system of homogeneous linear equations  $\mathbf{e}_{\pm}(\mathbf{A} -$   
 419  $\mu_{\pm} \text{id}) = 0$

$$420 \quad \begin{cases} (\mu_{\mp} + \gamma'_d)e_{\pm,u} & + \varepsilon\gamma' e_{\pm,d} = 0 \\ \gamma'_d e_{\pm,u} + [\mu_{\mp} - (\lambda' - \varepsilon\gamma')]e_{\pm,d} = 0 \end{cases}$$

421

422 I solve the first equation for the component  $e_{\pm,d}$ , and substitute this result on the second equation

$$423 \quad e_{\pm,d} = -\frac{\mu_{\mp} + \gamma'_d}{\varepsilon\gamma'} e_{\pm,u} \longrightarrow$$

$$424 \quad \left( \gamma'_d - \frac{[\mu_{\mp} - (\lambda' - \varepsilon\gamma')](\mu_{\mp} + \gamma'_d)}{\varepsilon\gamma'} \right) e_{\pm,u} = 0$$

$$425 \quad \frac{\varepsilon\gamma'\gamma'_d - [\mu_{\mp} - (\lambda' - \varepsilon\gamma')](\mu_{\mp} + \gamma'_d)}{\varepsilon\gamma'} e_{\pm,u} = 0, (\varepsilon, \gamma' \neq 0) \therefore$$

426  
427

$$428 \quad \{ \varepsilon\gamma'\gamma'_d - [\mu_{\mp} - (\lambda' - \varepsilon\gamma')](\mu_{\mp} + \gamma'_d) \} e_{\pm,u} = 0$$

$$429 \quad \{ \varepsilon\gamma'\gamma'_d + [(\lambda' - \varepsilon\gamma') - \mu_{\mp}](\gamma'_d + \mu_{\mp}) \} e_{\pm,u} = 0$$

$$430 \quad - \{ -\varepsilon\gamma'\gamma'_d + [(\lambda' - \varepsilon\gamma') - \mu_{\mp}](-\gamma'_d - \mu_{\mp}) \} e_{\pm,u} = 0$$

431

432 and in the last expression we have two options: either  $e_{\pm,u}$  is zero or the term within curly braces is  
 433 zero. However, the expression in curly braces is the characteristic equation (A5) and then always  
 434 vanishes identically. This means that  $e_{\pm,u} = \alpha \in \mathbb{R}$  can be chosen arbitrarily. I plug in this result in  
 435 the expression for  $e_{\pm,d}$  and get that

$$436 \quad e_{\pm,u} = \alpha$$

$$437 \quad e_{\pm,d} = -\frac{\mu_{\mp} + \gamma'_d}{\varepsilon\gamma'} \alpha$$

438

439 or as a vector in the temperature basis

$$\begin{aligned} 440 \quad \mathbf{e}_{\pm} &= e_{\pm,u} \mathbf{e}_u + e_{\pm,d} \mathbf{e}_d \\ 441 \quad \mathbf{e}_{\pm} &= \alpha \mathbf{e}_u - \frac{\mu_{\mp} + \gamma'_d}{\varepsilon \gamma'} \alpha \mathbf{e}_d \\ 442 \end{aligned}$$

443 and since  $\alpha$  is arbitrary this means we are in front of a subspace of vectors. I choose a basis by  
444 selecting  $\alpha = 1$ .

$$\begin{aligned} 445 \quad \mathbf{e}_{\pm} &= \mathbf{e}_u - \frac{\mu_{\mp} + \gamma'_d}{\varepsilon \gamma'} \mathbf{e}_d \\ 446 \end{aligned}$$

447 which is the same as the equation (A8).

448 Now, I can derive the expressions of the temperature basis vectors in terms of the two eigenvectors.

449 If one solves for  $e_u$  in equation (A8)

$$\begin{aligned} 450 \quad \mathbf{e}_{\pm} + \frac{\mu_{\mp} + \gamma'_d}{\varepsilon \gamma'} \mathbf{e}_d &= \mathbf{e}_u \\ 451 \end{aligned}$$

452 but we have here two expressions in a condensed way. Therefore,

$$\begin{aligned} 453 \quad \mathbf{e}_- + \frac{\mu_+ + \gamma'_d}{\varepsilon \gamma'} \mathbf{e}_d &= \mathbf{e}_+ + \frac{\mu_- + \gamma'_d}{\varepsilon \gamma'} \mathbf{e}_d \\ 454 \quad \left( \frac{\mu_+ + \gamma'_d}{\varepsilon \gamma'} - \frac{\mu_- + \gamma'_d}{\varepsilon \gamma'} \right) \mathbf{e}_d &= \mathbf{e}_+ - \mathbf{e}_- \\ 455 \quad \frac{(\mu_+ + \gamma'_d) - (\mu_- + \gamma'_d)}{\varepsilon \gamma'} \mathbf{e}_d &= \mathbf{e}_+ - \mathbf{e}_- \\ 456 \quad \frac{\mu_+ - \mu_-}{\varepsilon \gamma'} \mathbf{e}_d &= \mathbf{e}_+ - \mathbf{e}_- \\ 457 \quad \mathbf{e}_d &= \frac{\varepsilon \gamma'}{\mu_+ - \mu_-} (\mathbf{e}_+ - \mathbf{e}_-) \\ 458 \end{aligned}$$

459 Thus, I have expressed  $\mathbf{e}_d$  in terms of the eigenvectors.

Now, I substitute the last result on one of the expressions for  $\mathbf{e}_u$ .

$$\begin{aligned}
\mathbf{e}_+ + \frac{\mu_- + \gamma'_d}{\varepsilon\gamma'} \mathbf{e}_d &= \mathbf{e}_u \\
\mathbf{e}_+ + \frac{\mu_- + \gamma'_d}{\varepsilon\gamma'} \frac{\varepsilon\gamma'}{\mu_+ - \mu_-} (\mathbf{e}_+ - \mathbf{e}_-) &= \mathbf{e}_u \\
\mathbf{e}_+ + \frac{\mu_- + \gamma'_d}{\mu_+ - \mu_-} (\mathbf{e}_+ - \mathbf{e}_-) &= \mathbf{e}_u \\
\left(1 + \frac{\mu_- + \gamma'_d}{\mu_+ - \mu_-}\right) \mathbf{e}_+ - \frac{\mu_- + \gamma'_d}{\mu_+ - \mu_-} \mathbf{e}_- &= \mathbf{e}_u \\
\frac{\mu_+ - \mu_- + \mu_- + \gamma'_d}{\mu_+ - \mu_-} \mathbf{e}_+ - \frac{\mu_- + \gamma'_d}{\mu_+ - \mu_-} \mathbf{e}_- &= \mathbf{e}_u \\
\frac{\mu_+ + \gamma'_d}{\mu_+ - \mu_-} \mathbf{e}_+ - \frac{\mu_- + \gamma'_d}{\mu_+ - \mu_-} \mathbf{e}_- &= \mathbf{e}_u
\end{aligned}$$

and the temperature basis vectors in the eigenvector representation are

$$\begin{aligned}
\mathbf{e}_u &= \frac{\mu_+ + \gamma'_d}{\mu_+ - \mu_-} \mathbf{e}_+ - \frac{\mu_- + \gamma'_d}{\mu_+ - \mu_-} \mathbf{e}_- \\
\mathbf{e}_d &= \frac{\varepsilon\gamma'}{\mu_+ - \mu_-} (\mathbf{e}_+ - \mathbf{e}_-)
\end{aligned} \tag{A9}$$

### Matrix in the eigenvector representation. Solutions

With these results, I can write the matrix  $\mathbf{A}$  (A3) in the eigenvector basis and it should be the following diagonal matrix

$$\mathbf{B} = \begin{pmatrix} \mu_+ & 0 \\ 0 & \mu_- \end{pmatrix} \tag{A10}$$

I show how to get to this result. Let subscripts represent rows and superscripts represent columns.

I define that latin indices ( $i, j, k, \dots$ ) have the possible values u, d; and greek indices ( $\alpha, \beta, \zeta, \dots$ )

have possible values +, -. Also, repeated indices in expressions mean summation over the set of

possible values. With these considerations, equation (A9) is

$$\mathbf{e}_i = \Lambda_i^\alpha \mathbf{e}_\alpha$$

482 where the rows of matrix  $\Lambda$  contain the coordinates of each of the vectors of the temperature basis  
 483 in the eigenvector representation. Analogously, equation (A8) is

$$484 \quad \mathbf{e}_\alpha = \Theta_\alpha^i \mathbf{e}_i$$

486 where matrix  $\Theta$  has in its rows the coordinates the eigenvector basis in the temperature represen-  
 487 tation. This means that

$$488 \quad \mathbf{e}_\alpha = \Theta_\alpha^i \mathbf{e}_i = \Theta_\alpha^i \Lambda_i^\beta \mathbf{e}_\beta$$

490 which is only possible if the matrices  $\Lambda$  and  $\Theta$  are inverse of each other

$$491 \quad \mathbf{e}_\alpha = \delta_\alpha^\beta \mathbf{e}_\beta = \mathbf{e}_\alpha$$

493 Thus, we write  $\Theta = \Lambda^{-1}$ .

494 Now, matrix  $\mathbf{A}$  is the temperature representation of a linear operator  $f$ . If  $\mathbf{v} = v^j \mathbf{e}_j$  is a vector in  
 495 the temperature representation, then the action of the linear operator  $f$  should be  $f(\mathbf{v}) = f(v^j \mathbf{e}_j) =$   
 496  $v^j f(\mathbf{e}_j)$ . Then the action of  $f$  on a vector expressed in a given basis only depends on the action  
 497 of the operator on the basis:  $f(\mathbf{v}) = f(v^j \mathbf{e}_j) = v^j f(\mathbf{e}_j) = v^j \mathbf{A}_j^k \mathbf{e}_k$ . Thus, the matrix  $\mathbf{A}$  has in its  
 498 rows the coordinates in the temperature representation of the action of  $f$  over each basis vector.  
 499 Once one understands what is happening under the hood, what we want is the matrix  $\mathbf{B}$ , which  
 500 is the representation of  $f$  in the eigenvector basis. Therefore, I begin with the basic relationship  
 501 in the temperature representation and introduce the change of representation using the alternative

502 representation of equations (A8) and (A9)

$$503 \quad f(\mathbf{e}_i) = \mathbf{A}_i^j \Lambda_j^\zeta \mathbf{e}_\zeta$$

$$504 \quad f(\Lambda_i^\alpha \mathbf{e}_\alpha) = \mathbf{A}_i^j \Lambda_j^\zeta \mathbf{e}_\zeta$$

$$505 \quad \Lambda_i^\alpha f(\mathbf{e}_\alpha) = \mathbf{A}_i^j \Lambda_j^\zeta \mathbf{e}_\zeta$$

$$506 \quad (\Lambda^{-1})_\beta^i \Lambda_i^\alpha f(\mathbf{e}_\alpha) = (\Lambda^{-1})_\beta^i \mathbf{A}_i^j \Lambda_j^\zeta \mathbf{e}_\zeta$$

$$507 \quad f(\mathbf{e}_\beta) = (\Lambda^{-1})_\beta^i \mathbf{A}_i^j \Lambda_j^\zeta \mathbf{e}_\zeta, f(\mathbf{e}_\beta) := \mathbf{B}_\beta^\zeta \mathbf{e}_\zeta$$

$$508 \quad \mathbf{B}_\beta^\zeta = (\Lambda^{-1})_\beta^i \mathbf{A}_i^j \Lambda_j^\zeta$$

510 or in matrix notation  $\mathbf{B} = \Lambda^{-1} \mathbf{A} \Lambda$ . Then, I multiply the matrices

$$511 \quad \Lambda^{-1} = \begin{pmatrix} 1 & -\frac{\mu_- + \gamma'_d}{\varepsilon \gamma'} \\ 1 & -\frac{\mu_+ + \gamma'_d}{\varepsilon \gamma'} \end{pmatrix}, \mathbf{A} = \begin{pmatrix} \hat{\lambda} + \gamma'_d & \gamma'_d \\ \varepsilon \gamma' & -\gamma'_d \end{pmatrix}, \Lambda = \begin{pmatrix} \frac{\mu_+ + \gamma'_d}{\mu_+ - \mu_-} & -\frac{\mu_- + \gamma'_d}{\mu_+ - \mu_-} \\ \frac{\varepsilon \gamma'}{\mu_+ - \mu_-} & -\frac{\varepsilon \gamma'}{\mu_+ - \mu_-} \end{pmatrix}$$

513 First, note that  $\mu_+ - \mu_- = \kappa$ . One also looks at the following quantities that will help in the  
514 process:  $\mu_+ + \mu_- = \hat{\lambda}$  and  $\mu_+ \mu_- = \frac{1}{4}(\hat{\lambda}^2 - \kappa^2) = \frac{1}{4}(\hat{\lambda}^2 - \hat{\lambda}^2 - 4\lambda' \gamma'_d) = -\lambda' \gamma'_d$ . I proceed with the first  
515 product,  $\Lambda^{-1} \mathbf{A}$ .

$$516 \quad \Lambda^{-1} \mathbf{A} = \begin{pmatrix} 1 & -\frac{\mu_- + \gamma'_d}{\varepsilon \gamma'} \\ 1 & -\frac{\mu_+ + \gamma'_d}{\varepsilon \gamma'} \end{pmatrix} \begin{pmatrix} \hat{\lambda} + \gamma'_d & \gamma'_d \\ \varepsilon \gamma' & -\gamma'_d \end{pmatrix}$$

$$517 \quad = \begin{pmatrix} \hat{\lambda} + \gamma'_d - \mu_- - \gamma'_d & \left(1 + \frac{\mu_- + \gamma'_d}{\varepsilon \gamma'}\right) \gamma'_d \\ \hat{\lambda} + \gamma'_d - \mu_+ - \gamma'_d & \left(1 + \frac{\mu_+ + \gamma'_d}{\varepsilon \gamma'}\right) \gamma'_d \end{pmatrix}$$

$$518 \quad = \begin{pmatrix} \hat{\lambda} - \mu_- & \frac{\varepsilon \gamma' + \mu_- + \gamma'_d}{\varepsilon \gamma'} \gamma'_d \\ \hat{\lambda} - \mu_+ & \frac{\varepsilon \gamma' + \mu_+ + \gamma'_d}{\varepsilon \gamma'} \gamma'_d \end{pmatrix}$$

$$519 \quad = \begin{pmatrix} \mu_+ & \frac{\varepsilon \gamma' + \mu_- + \gamma'_d}{\varepsilon \gamma'} \gamma'_d \\ \mu_- & \frac{\varepsilon \gamma' + \mu_+ + \gamma'_d}{\varepsilon \gamma'} \gamma'_d \end{pmatrix}$$

520

521 and multiply the result by  $\Lambda$

$$\begin{aligned}
522 \quad \Lambda^{-1} \mathbf{A} \Lambda &= \begin{pmatrix} \mu_+ & \frac{\varepsilon \gamma' + \mu_- + \gamma'_d}{\varepsilon \gamma'} \gamma'_d \\ \mu_- & \frac{\varepsilon \gamma' + \mu_+ + \gamma'_d}{\varepsilon \gamma'} \gamma'_d \end{pmatrix} \begin{pmatrix} \frac{\mu_+ + \gamma'_d}{\mu_+ - \mu_-} & -\frac{\mu_- + \gamma'_d}{\mu_+ - \mu_-} \\ \frac{\varepsilon \gamma'}{\mu_+ - \mu_-} & -\frac{\varepsilon \gamma'}{\mu_+ - \mu_-} \end{pmatrix} \\
523 \quad &= \frac{1}{\kappa} \begin{pmatrix} \mu_+^2 + \mu_+ \gamma'_d + \varepsilon \gamma' \gamma'_d + \mu_- \gamma'_d + \gamma'_d{}^2 & -\mu_+ \mu_- - \mu_+ \gamma'_d - \varepsilon \gamma' \gamma'_d - \mu_- \gamma'_d - \gamma'_d{}^2 \\ \mu_- \mu_+ + \mu_- \gamma'_d + \varepsilon \gamma' \gamma'_d + \mu_+ \gamma'_d + \gamma'_d{}^2 & -\mu_-^2 - \mu_- \gamma'_d - \varepsilon \gamma' \gamma'_d - \mu_+ \gamma'_d - \gamma'_d{}^2 \end{pmatrix} \\
524 \quad &= \frac{1}{\kappa} \begin{pmatrix} \mu_+^2 + (\hat{\lambda} + \varepsilon \gamma' + \gamma'_d) \gamma'_d & -\mu_+ \mu_- - (\hat{\lambda} + \varepsilon \gamma' + \gamma'_d) \gamma'_d \\ \mu_- \mu_+ + (\hat{\lambda} + \varepsilon \gamma' + \gamma'_d) \gamma'_d & -\mu_-^2 - (\hat{\lambda} + \varepsilon \gamma' + \gamma'_d) \gamma'_d \end{pmatrix} \\
525 \quad &= \frac{1}{\kappa} \begin{pmatrix} \mu_+^2 - \mu_+ \mu_- & \lambda' \gamma'_d - \lambda \gamma'_d \\ -\lambda' \gamma'_d + \lambda \gamma'_d & -\mu_-^2 + \mu_+ \mu_- \end{pmatrix} = \frac{1}{\kappa} \begin{pmatrix} \mu_+ \kappa & 0 \\ 0 & \mu_- \kappa \end{pmatrix} = \begin{pmatrix} \mu_+ & 0 \\ 0 & \mu_- \end{pmatrix} \\
526 \quad & \\
527 \quad &
\end{aligned}$$

527 the last line is the result that we wanted to check.

528 In the eigenvector representation the system (A4) has the following form

$$529 \quad \dot{\mathbf{T}} = \mathbf{F}' + \mathbf{T} \mathbf{B} \quad (A11)$$

531 and, therefore, is decoupled. Therefore, I can solve each equation separately. I only need to  
532 transform the forcing vector to the eigenvector representation.

533 The equations are

$$534 \quad \dot{T}_{\pm} = F'_{\pm} + \mu_{\pm} T_{\pm}$$

536 and the solutions of a generic initial value problem are

$$537 \quad T_{\pm} = \left( T_{\pm,0} + \int_{t_0}^t F'_{\pm} e^{-\mu_{\pm}(\tau-t_0)} d\tau \right) e^{\mu_{\pm}(t-t_0)} \quad (A12)$$

539 where the initial values in the eigenvector representation in terms of the initial values in the  
540 temperature representation are

$$541 \quad T_{\pm,0} = \pm \frac{1}{\mu_+ - \mu_-} [(\mu_{\pm} + \gamma'_d) T_{u,0} + \varepsilon \gamma' T_{d,0}]$$

543 the forcing components are

$$544 \quad F'_\pm = \pm \frac{\mu_\pm + \gamma'_d}{\mu_+ - \mu_-} F'$$

545

546 and the solutions in the temperature representation are

$$547 \quad T_u = T_+ + T_-$$

$$548 \quad T_d = -\frac{\mu_- + \gamma'_d}{\varepsilon\gamma'} T_+ - \frac{\mu_+ + \gamma'_d}{\varepsilon\gamma'} T_-$$

549 If I further expand the  $T_d$  solution, the form of the solutions is more elegant

$$550 \quad T_u = T_+ + T_- \tag{A13}$$

$$551 \quad T_d = -\frac{\hat{\lambda} + 2\gamma'_d}{2\varepsilon\gamma'} (T_+ + T_-) + \frac{\kappa}{2\varepsilon\gamma'} (T_+ - T_-)$$

552 since it shows that the solutions in the temperature space are in a sort of symmetric and antisymmet-  
553 ric combinations of the solutions in the eigenvector representation. These are the normal modes.

554 One thing to note is that the upper temperature is the symmetric mode and the deep temperature is  
555 a mixture of symmetric and antisymmetric modes.

556 I show how I got the solutions (A13). Just expand the  $T_d$  equation.

$$557 \quad T_d = -\frac{\mu_- + \gamma'_d}{\varepsilon\gamma'} T_+ - \frac{\mu_+ + \gamma'_d}{\varepsilon\gamma'} T_-$$

$$558 \quad = -\frac{1}{\varepsilon\gamma'} \left[ \left( \frac{\hat{\lambda} - \kappa}{2} + \gamma'_d \right) T_+ + \left( \frac{\hat{\lambda} + \kappa}{2} + \gamma'_d \right) T_- \right]$$

$$559 \quad = -\frac{1}{\varepsilon\gamma'} \left[ \left( \frac{\hat{\lambda} + 2\gamma'_d}{2} - \frac{\kappa}{2} \right) T_+ + \left( \frac{\hat{\lambda} + 2\gamma'_d}{2} + \frac{\kappa}{2} \right) T_- \right]$$

$$560 \quad = -\frac{1}{2\varepsilon\gamma'} [(\hat{\lambda} + 2\gamma'_d)(T_+ + T_-) - \kappa(T_+ - T_-)]$$

561

562 From now on, I write  $T_s := T_+ + T_-$  and  $T_a := T_+ - T_-$ .

563 **Planetary imbalance**

564 Now, I will find an expression for the planetary imbalance in terms of the equations (A13). The

565 mathematical expression that I should expand is  $N = N_u + N_d = C_u \dot{T}_u + C_d \dot{T}_d$

$$\begin{aligned}
 566 \quad C_u \dot{T}_u &= C_u \dot{T}_s \\
 567 \quad C_d \dot{T}_d &= -C_d \frac{\hat{\lambda} + 2\gamma'_d}{2\varepsilon\gamma'} \dot{T}_s + C_d \frac{\kappa}{2\varepsilon\gamma'} \dot{T}_a \therefore \\
 568 \quad N &= C_u \dot{T}_s - C_d \frac{\hat{\lambda} + 2\gamma'_d}{2\varepsilon\gamma'} \dot{T}_s + C_d \frac{\kappa}{2\varepsilon\gamma'} \dot{T}_a \\
 569 \quad &= \left( C_u - C_d \frac{\hat{\lambda} + 2\gamma'_d}{2\varepsilon\gamma'} \right) \dot{T}_s + C_d \frac{\kappa}{2\varepsilon\gamma'} \dot{T}_a \\
 570 \quad &= C_s \dot{T}_s + C_a \dot{T}_a \\
 571
 \end{aligned}$$

572 Now,  $\dot{T}_\pm = F'_\pm + \mu_\pm T_\pm$ , then

$$\begin{aligned}
 573 \quad \dot{T}_s &= \mu_+ T_+ + \mu_- T_- + (F'_+ + F'_-) = \mu_+ T_+ + (\mu_+ - \kappa) T_- + (F'_+ + F'_-) \\
 574 \quad &= \mu_+ T_s - \kappa T_- + (F'_+ + F'_-) = \mu_+ T_s - \frac{\kappa}{2} (T_s - T_a) + (F'_+ + F'_-) \\
 575 \quad &= \frac{\hat{\lambda}}{2} T_s + \frac{\kappa}{2} T_a + (F'_+ + F'_-) = \frac{\hat{\lambda}}{2} T_s + \frac{\kappa}{2} T_a + F' \\
 576 \quad \dot{T}_a &= \mu_+ T_+ - \mu_- T_- + (F'_+ - F'_-) = \mu_+ T_+ - (\mu_+ - \kappa) T_- + (F'_+ - F'_-) \\
 577 \quad &= \mu_+ T_a + \kappa T_- + (F'_+ - F'_-) = \mu_+ T_a + \frac{\kappa}{2} (T_s - T_a) + (F'_+ - F'_-) \\
 578 \quad &= \frac{\kappa}{2} T_s + \frac{\hat{\lambda}}{2} T_a + (F'_+ - F'_-) = \frac{\kappa}{2} T_s + \frac{\hat{\lambda}}{2} T_a + \frac{\hat{\lambda} + 2\gamma'_d}{\kappa} F' \therefore \\
 579 \quad N &= \frac{1}{2} (\hat{\lambda} C_s + \kappa C_a) T_s + \frac{1}{2} (\hat{\lambda} C_a + \kappa C_s) T_a + \left( C_s + C_a \frac{\hat{\lambda} + 2\gamma'_d}{\kappa} \right) F' \\
 580
 \end{aligned}$$

Further expanding the coefficients

$$\begin{aligned}
\hat{\lambda}C_s + \kappa C_a &= \hat{\lambda}C_u - \frac{C_d}{2\varepsilon\gamma'}(\hat{\lambda}^2 + 2\gamma'_d\hat{\lambda} - \kappa^2) = \hat{\lambda}C_u - \frac{C_d}{2\varepsilon\gamma'}(\hat{\lambda}^2 + 2\gamma'_d\hat{\lambda} - \hat{\lambda}^2 - 4\gamma'_d\lambda') \\
&= 2\frac{C_u}{\varepsilon}\left(\lambda' + \frac{\varepsilon-1}{2}\hat{\lambda}\right) \\
\hat{\lambda}C_a + \kappa C_s &= \kappa C_u - \frac{C_d}{2\varepsilon\gamma'}(\kappa\hat{\lambda} + 2\gamma'_d\kappa - \kappa\hat{\lambda}) = \kappa C_u - \frac{C_u}{\varepsilon}\kappa = \kappa\frac{C_u}{\varepsilon}(\varepsilon-1) \\
C_s + C_a\frac{\hat{\lambda} + 2\gamma'_d}{\kappa} &= C_u - \frac{C_d}{2\varepsilon\gamma'}(\hat{\lambda} + 2\gamma'_d - \hat{\lambda} - 2\gamma'_d) = C_u
\end{aligned}$$

then the imbalance is

$$N = \frac{C_u}{\varepsilon}\left[\varepsilon F' + \left(\lambda' + \frac{\varepsilon-1}{2}\hat{\lambda}\right)T_s + \kappa\frac{\varepsilon-1}{2}T_a\right] \quad (\text{A14})$$

From here, I derive the slope of a  $NT$ -diagram. In such a diagram,  $N$  is plotted versus  $T_u$ . If we naively take the partial derivative of equation (A14) with respect to  $T_u$ , we will arrive to a constant slope. This is contrary to the evidence that it will change with time. An  $NT$ -diagram is one projection of the phase space of the system. Then, the  $NT$ -diagram slope does not only depend on how  $N$  varies with  $T_u$ . It is a comparison of how the changes of  $T_u$  are expressed in changes of  $N$ . Then, the slope is the total derivative  $dN/dT_u$ . By virtue of the chain rule,  $dN/dT_u = \dot{N}(dt/dT_u)$ . In a neighborhood where  $T_u(t)$  is injective,  $dt/dT_u = 1/\dot{T}_u$ . Therefore, the slope  $dN/dT_u$  is the ratio of two total derivatives:  $\dot{N}$  and  $\dot{T}_u$ .

We know that  $T_u = T_s$ , then  $\dot{T}_u = \dot{T}_s$ . Therefore, the total derivative of the planetary imbalance is

$$\dot{N} = (\partial_t N) + (\partial_{T_s} N)\dot{T}_s + (\partial_{T_a} N)\dot{T}_a$$

that is a change depending only on time, a second change depending only on changes of  $T_s$  and a third depending on changes of  $T_a$ . Therefore, the ratio of total derivative of planetary imbalance and total derivative of  $T_u$  is

$$\frac{\dot{N}}{\dot{T}_u} = (\partial_t N)\frac{1}{\dot{T}_s} + (\partial_{T_s} N) + (\partial_{T_a} N)\frac{\dot{T}_a}{\dot{T}_s}$$

606 As one can see in the above expression, the ratio includes the derivative of the imbalance with  
607 respect to  $T_u$  but is not the only contribution. One contribution comes from the explicit dependence  
608 on time of  $N$  and how it compares with the dependency of  $T_u$ . The other contribution comes  
609 from the antisymmetric mode and how it changes in relation to the symmetric one. From equation  
610 (A14), I can write the precise expression of the slope as a factor of  $\lambda$ .

611 I multiply equation (A14) by  $\lambda/\lambda$  and reorganise.

$$\begin{aligned}
612 \quad \frac{\dot{N}}{\dot{T}_u} &= \frac{C_u}{\varepsilon} \left[ \varepsilon \frac{\dot{F}'}{\dot{T}_s} + \left( \lambda' + \frac{\varepsilon-1}{2} \hat{\lambda} \right) + \kappa \frac{\varepsilon-1}{2} \frac{\dot{T}_a}{\dot{T}_s} \right] \frac{\lambda}{\lambda} \\
613 \quad &= \left[ \frac{C_u \dot{F}'}{\lambda \dot{T}_s} + \left( \frac{\lambda'}{\varepsilon \lambda} + \frac{\varepsilon-1}{2\varepsilon} \frac{\hat{\lambda}}{\lambda'} \right) + \frac{\varepsilon-1}{2\varepsilon} \frac{\kappa \dot{T}_a}{\lambda' \dot{T}_s} \right] \lambda
\end{aligned}$$

615 then we will expand the terms to separate the terms that vanish when  $\varepsilon = 1$

$$\begin{aligned}
616 \quad \frac{\dot{N}}{\dot{T}_u} &= \left\{ \frac{C_u \dot{F}'}{\lambda \dot{T}_s} + \left[ \frac{1}{\varepsilon} + \frac{\varepsilon-1}{2\varepsilon} \left( \frac{\lambda' - \varepsilon \gamma' - \gamma'_d}{\lambda'} \right) \right] + \frac{\varepsilon-1}{2\varepsilon} \frac{\kappa \dot{T}_a}{\lambda' \dot{T}_s} \right\} \lambda \\
617 \quad &= \left\{ \frac{C_u \dot{F}'}{\lambda \dot{T}_s} + \left[ \frac{2}{2\varepsilon} + \frac{\varepsilon-1}{2\varepsilon} \left( 1 - \varepsilon \frac{\gamma}{\lambda} - \frac{C_u \gamma}{C_d \lambda} \right) \right] + \frac{\varepsilon-1}{2\varepsilon} \frac{C_u \kappa \dot{T}_a}{\lambda \dot{T}_s} \right\} \lambda \\
618 \quad &= \left[ \frac{C_u \dot{F}'}{\lambda \dot{T}_s} + \frac{\varepsilon+1}{2\varepsilon} - \frac{\varepsilon-1}{2\varepsilon} \left( \varepsilon + \frac{C_u}{C_d} \right) \frac{\gamma}{\lambda} + \frac{\varepsilon-1}{2\varepsilon} \frac{C_u \kappa \dot{T}_a}{\lambda \dot{T}_s} \right] \lambda \\
619 \quad &= \left[ \frac{C_u \dot{F}'}{\lambda \dot{T}_s} + \frac{\varepsilon+1}{2\varepsilon} - \frac{\varepsilon-1}{2\varepsilon} \left( \varepsilon + \frac{C_u}{C_d} \right) \frac{\gamma}{\lambda} + \frac{\varepsilon-1}{2\varepsilon} \frac{C_u \kappa \dot{T}_a}{\lambda \dot{T}_s} \right] \lambda \\
620 \quad &= \left\{ \frac{C_u \dot{F}'}{\lambda \dot{T}_s} + \frac{\varepsilon+1}{2\varepsilon} - \frac{\varepsilon-1}{2\varepsilon \lambda} \left[ \left( \varepsilon + \frac{C_u}{C_d} \right) \gamma - C_u \kappa \frac{\dot{T}_a}{\dot{T}_s} \right] \right\} \lambda \\
621 \quad &= \left\{ \frac{C_u \dot{F}'}{\lambda \dot{T}_s} + \frac{\varepsilon+1}{2\varepsilon} - \frac{\varepsilon-1}{2\varepsilon \lambda} C_u \kappa \left[ \left( \varepsilon + \frac{C_u}{C_d} \right) \frac{\gamma}{C_u \kappa} - \frac{\dot{T}_a}{\dot{T}_s} \right] \right\} \lambda \\
622 \quad &= \left\{ \frac{C_u \dot{F}'}{\lambda \dot{T}_s} + \frac{\varepsilon+1}{2\varepsilon} - \frac{\varepsilon-1}{2\varepsilon} \frac{C_u \kappa}{\lambda} \left[ \left( \varepsilon + \frac{C_u}{C_d} \right) \frac{\gamma}{C_u \kappa} - \frac{\dot{T}_a}{\dot{T}_s} \right] \right\} \lambda \\
623 \quad &= \left\{ -\frac{C_u \dot{F}'}{|\lambda| \dot{T}_s} + \frac{\varepsilon+1}{2\varepsilon} + \frac{\varepsilon-1}{2\varepsilon} \frac{C_u \kappa}{|\lambda|} \left[ \left( \varepsilon + \frac{C_u}{C_d} \right) \frac{\gamma}{C_u \kappa} - \frac{\dot{T}_a}{\dot{T}_s} \right] \right\} \lambda \\
624 \quad & \\
625 \quad & \\
626 \quad \frac{\dot{N}}{\dot{T}_u} &= \left\{ -\frac{C_u \dot{F}'}{|\lambda| \dot{T}_s} + \frac{\varepsilon+1}{2\varepsilon} \left( 1 + \frac{\varepsilon-1}{\varepsilon+1} \frac{C_u \kappa}{|\lambda|} \left[ \left( \varepsilon + \frac{C_u}{C_d} \right) \frac{\gamma}{C_u \kappa} - \frac{\dot{T}_a}{\dot{T}_s} \right] \right) \right\} \lambda \quad (A15) \\
627 \quad &
\end{aligned}$$

628 The term in square brackets in equation (A15) is the key term that provides a  $NT$ -diagram with  
629 evolving slope when the forcing is constant. The second part of this term provides the temporal

630 evolution, whereas the first part is a constant term that sets the base enhancement of the slope.  
 631 Interestingly, this first part contains in particular the thermal capacities of the system.

632 If I rewrite this first part of the square-brackets term, the terms are shown clearly

$$633 \quad \frac{\dot{N}}{\dot{T}_u} = \left\{ -\frac{C_u \dot{F}'}{|\lambda| \dot{T}_s} + \frac{\varepsilon + 1}{2\varepsilon} + \frac{\varepsilon - 1}{2\varepsilon} \frac{C_u \kappa}{|\lambda|} \left[ \left( \frac{\varepsilon}{C_u} + \frac{1}{C_d} \right) \frac{\gamma}{\kappa} - \frac{\dot{T}_a}{\dot{T}_s} \right] \right\} \lambda \quad (A16)$$

634

635 Now in the first part it is the sum of the inverse of the thermal capacities as if we have an electrical  
 636 circuit with capacitors in series. Having such a term in the equation for the slope favors the physical  
 637 interpretation in terms of thermal capacities, instead of variable feedback mechanisms. The time-  
 638 evolving ratio term in the second part, that represents the dynamics of the atmosphere-ocean  
 639 coupling, only strengthens this interpretation.

640 As a corollary, if the forcing is constant and  $\varepsilon \rightarrow 1$ , then we recover the classical linear dependence  
 641 of the imbalance on  $T_u$

$$642 \quad \lim_{\varepsilon \rightarrow 1} \frac{\dot{N}}{\dot{T}_u} = \lambda, F = \text{const}$$

643

## 644 **Symmetric and antisymmetric modes**

645 From equations (A13), we see that the symmetric and antisymmetric modes are the basis for  
 646 the description of the solutions. Thus, let us give some explicit expression for the symmetric and  
 647 antisymmetric modes.



670  $\cosh x \pm \sinh x$ . The factors within square brackets in the last two terms can be thought as  $e^x I_+ \pm$   
671  $e^{-x} I_-$ , where  $I_{\pm}$  are the corresponding integrals. Using the expression of the exponential function in  
672 terms of the hyperbolic functions, I expand  $e^x I_+ \pm e^{-x} I_- = (\cosh x + \sinh x) I_+ \pm (\cosh x - \sinh x) I_- =$   
673  $(I_+ \pm I_-) \cosh x + (I_+ \mp I_-) \sinh x$ . Then, I overcome the limitation and now the two terms are written  
674 with hyperbolic functions. The coefficients of the hyperbolic functions are simple combinations  
675 of the integrals which can be also expanded easily. I do that now

$$\begin{aligned}
676 \quad I_+ + I_- &= \int_{t_0}^t F' e^{-\mu_+(\tau-t_0)} d\tau + \int_{t_0}^t F' e^{-\mu_-(\tau-t_0)} d\tau = \int_{t_0}^t F' [e^{-\mu_+(\tau-t_0)} + e^{-\mu_-(\tau-t_0)}] d\tau \\
677 \quad &= \int_{t_0}^t F' e^{-(\hat{\lambda}/2)(\tau-t_0)} [e^{-(\kappa/2)(\tau-t_0)} + e^{(\kappa/2)(\tau-t_0)}] d\tau \\
678 \quad &= 2 \int_{t_0}^t F' e^{-(\hat{\lambda}/2)(\tau-t_0)} \cosh \left[ \frac{\kappa}{2}(\tau-t_0) \right] d\tau \\
679 \quad I_+ - I_- &= \int_{t_0}^t F' e^{-\mu_+(\tau-t_0)} d\tau - \int_{t_0}^t F' e^{-\mu_-(\tau-t_0)} d\tau = \int_{t_0}^t F' [e^{-\mu_+(\tau-t_0)} - e^{-\mu_-(\tau-t_0)}] d\tau \\
680 \quad &= \int_{t_0}^t F' e^{-(\hat{\lambda}/2)(\tau-t_0)} [e^{-(\kappa/2)(\tau-t_0)} - e^{(\kappa/2)(\tau-t_0)}] d\tau \\
681 \quad &= -2 \int_{t_0}^t F' e^{-(\hat{\lambda}/2)(\tau-t_0)} \sinh \left[ \frac{\kappa}{2}(\tau-t_0) \right] d\tau \\
682
\end{aligned}$$

683 If one collects terms corresponding to each hyperbolic function in the former expressions for the  
684 normal modes, obtains the following

$$685 \quad T_s = \frac{e^{(\hat{\lambda}/2)(t-t_0)}}{\kappa} \left\{ C_1 \cosh \left[ \frac{\kappa}{2}(t-t_0) \right] + C_2 \sinh \left[ \frac{\kappa}{2}(t-t_0) \right] \right\} \quad (\text{A17})$$

$$686 \quad T_a = \frac{e^{(\hat{\lambda}/2)(t-t_0)}}{\kappa} \left\{ C_2 \cosh \left[ \frac{\kappa}{2}(t-t_0) \right] + C_1 \sinh \left[ \frac{\kappa}{2}(t-t_0) \right] \right\} \quad (\text{A18})$$

688 where

$$689 \quad C_1 = \kappa T_{u,0}$$

$$690 \quad -(\hat{\lambda} + 2\gamma'_d) \int_{t_0}^t F' e^{-(\hat{\lambda}/2)(\tau-t_0)} \sinh \left[ \frac{\kappa}{2}(\tau - t_0) \right] d\tau + \kappa \int_{t_0}^t F' e^{-(\hat{\lambda}/2)(\tau-t_0)} \cosh \left[ \frac{\kappa}{2}(\tau - t_0) \right] d\tau$$

$$691 \quad C_2 = (\hat{\lambda} + 2\gamma'_d) T_{u,0} + 2\varepsilon\gamma'_d T_{d,0}$$

$$692 \quad + (\hat{\lambda} + 2\gamma'_d) \int_{t_0}^t F' e^{-(\hat{\lambda}/2)(\tau-t_0)} \cosh \left[ \frac{\kappa}{2}(\tau - t_0) \right] d\tau - \kappa \int_{t_0}^t F' e^{-(\hat{\lambda}/2)(\tau-t_0)} \sinh \left[ \frac{\kappa}{2}(\tau - t_0) \right] d\tau$$

694 These expressions for the normal modes are quite elegant, and the coefficients  $C_i$  summarize  
695 all the information from the initial conditions and the forcing. The initial condition terms in the  
696  $C_i$  correspond to the non-forced response of the system, while the part that is forcing-dependent  
697 corresponds to the forced response of the system.

### 698 **Forced response to constant forcing**

699 If  $F' = F'_c \neq 0$  for  $t > t_0$  with  $F'_c$  constant and  $T_{u,0}, T_{d,0} = 0$  for  $t = t_0$ , then

$$700 \quad C_1 = F'_c \left\{ -(\hat{\lambda} + 2\gamma'_d) \int_{t_0}^t e^{-(\hat{\lambda}/2)(\tau-t_0)} \sinh \left[ \frac{\kappa}{2}(\tau - t_0) \right] d\tau + \kappa \int_{t_0}^t e^{-(\hat{\lambda}/2)(\tau-t_0)} \cosh \left[ \frac{\kappa}{2}(\tau - t_0) \right] d\tau \right\}$$

$$701 \quad C_2 = F'_c \left\{ (\hat{\lambda} + 2\gamma'_d) \int_{t_0}^t e^{-(\hat{\lambda}/2)(\tau-t_0)} \cosh \left[ \frac{\kappa}{2}(\tau - t_0) \right] d\tau - \kappa \int_{t_0}^t e^{-(\hat{\lambda}/2)(\tau-t_0)} \sinh \left[ \frac{\kappa}{2}(\tau - t_0) \right] d\tau \right\}$$

703 where the integrals are easily computed

$$704 \quad \int_{t_0}^t e^{-(\hat{\lambda}/2)(\tau-t_0)} \sinh \left[ \frac{\kappa}{2}(\tau - t_0) \right] d\tau = \frac{e^{-(\hat{\lambda}/2)(t-t_0)}}{\lambda'\gamma'_d} \left\{ \frac{\kappa}{2} \cosh \left[ \frac{\kappa}{2}(t - t_0) \right] + \frac{\hat{\lambda}}{2} \sinh \left[ \frac{\kappa}{2}(t - t_0) \right] \right\} - \frac{\kappa}{2\lambda'\gamma'_d}$$

$$705 \quad \int_{t_0}^t e^{-(\hat{\lambda}/2)(\tau-t_0)} \cosh \left[ \frac{\kappa}{2}(\tau - t_0) \right] d\tau = \frac{e^{-(\hat{\lambda}/2)(t-t_0)}}{\lambda'\gamma'_d} \left\{ \frac{\hat{\lambda}}{2} \cosh \left[ \frac{\kappa}{2}(t - t_0) \right] + \frac{\kappa}{2} \sinh \left[ \frac{\kappa}{2}(t - t_0) \right] \right\} - \frac{\hat{\lambda}}{2\lambda'\gamma'_d}$$

707 and, upon reduction, the  $C_i$  are

$$708 \quad C_1 = \frac{F'_c}{\lambda'} e^{-(\hat{\lambda}/2)(\tau-t_0)} \left\{ -\kappa \cosh \left[ \frac{\kappa}{2}(t - t_0) \right] + (2\lambda' - \hat{\lambda}) \sinh \left[ \frac{\kappa}{2}(t - t_0) \right] + \kappa e^{(\hat{\lambda}/2)(t-t_0)} \right\}$$

$$709 \quad C_2 = \frac{F'_c}{\lambda'} e^{-(\hat{\lambda}/2)(\tau-t_0)} \left\{ -(2\lambda' - \hat{\lambda}) \cosh \left[ \frac{\kappa}{2}(t - t_0) \right] + \kappa \sinh \left[ \frac{\kappa}{2}(t - t_0) \right] + (2\lambda' - \hat{\lambda}) e^{(\hat{\lambda}/2)(t-t_0)} \right\}$$

710

711 with these expressions is easy to evaluate the terms inside the curly brackets in equations (A17)  
 712 and (A18) and the symmetric and antisymmetric modes are (for  $t \geq t_0$ )

$$713 \quad T_s = \frac{F_c}{\lambda} \left\{ e^{(\hat{\lambda}/2)(t-t_0)} \left( \cosh \left[ \frac{\kappa}{2}(t-t_0) \right] + \frac{2\lambda' - \hat{\lambda}}{\kappa} \sinh \left[ \frac{\kappa}{2}(t-t_0) \right] \right) - 1 \right\} \quad (\text{A19})$$

$$714 \quad T_a = \frac{F_c}{\lambda} \left\{ e^{(\hat{\lambda}/2)(t-t_0)} \left( \frac{2\lambda' - \hat{\lambda}}{\kappa} \cosh \left[ \frac{\kappa}{2}(t-t_0) \right] + \sinh \left[ \frac{\kappa}{2}(t-t_0) \right] \right) - \frac{2\lambda' - \hat{\lambda}}{\kappa} \right\} \quad (\text{A20})$$

716 where  $F'_c := F_c/C_u$ . I can also obtain the explicit time derivatives of both modes. We take the time  
 717 derivative both equations (A19) and (A20)

$$\begin{aligned} 718 \quad \dot{T}_s &= \frac{F_c}{\lambda} e^{(\hat{\lambda}/2)(t-t_0)} \left\{ \hat{\lambda} \left( \cosh \left[ \frac{\kappa}{2}(t-t_0) \right] + \frac{2\lambda' - \hat{\lambda}}{\kappa} \sinh \left[ \frac{\kappa}{2}(t-t_0) \right] \right) \right. \\ 719 &\quad \left. + \frac{\kappa}{2} \left( \frac{2\lambda' - \hat{\lambda}}{\kappa} \cosh \left[ \frac{\kappa}{2}(t-t_0) \right] + \sinh \left[ \frac{\kappa}{2}(t-t_0) \right] \right) \right\} \\ 720 &= \frac{F_c}{\lambda} e^{(\hat{\lambda}/2)(t-t_0)} \left\{ \lambda' \cosh \left[ \frac{\kappa}{2}(t-t_0) \right] + \frac{\lambda' \hat{\lambda} + 2\gamma'_d \lambda'}{\kappa} \sinh \left[ \frac{\kappa}{2}(t-t_0) \right] \right\} \\ 721 &= \frac{F_c}{C_u} e^{(\hat{\lambda}/2)(t-t_0)} \left\{ \cosh \left[ \frac{\kappa}{2}(t-t_0) \right] + \frac{\hat{\lambda} + 2\gamma'_d}{\kappa} \sinh \left[ \frac{\kappa}{2}(t-t_0) \right] \right\} \\ 722 \quad \dot{T}_a &= \frac{F_c}{\lambda} e^{(\hat{\lambda}/2)(t-t_0)} \left\{ \hat{\lambda} \left( \frac{2\lambda' - \hat{\lambda}}{\kappa} \cosh \left[ \frac{\kappa}{2}(t-t_0) \right] + \sinh \left[ \frac{\kappa}{2}(t-t_0) \right] \right) \right. \\ 723 &\quad \left. + \frac{\kappa}{2} \left( \cosh \left[ \frac{\kappa}{2}(t-t_0) \right] + \frac{2\lambda' - \hat{\lambda}}{\kappa} \sinh \left[ \frac{\kappa}{2}(t-t_0) \right] \right) \right\} \\ 724 &= \frac{F_c}{\lambda} e^{(\hat{\lambda}/2)(t-t_0)} \left\{ \frac{\lambda' \hat{\lambda} + 2\gamma'_d \lambda'}{\kappa} \cosh \left[ \frac{\kappa}{2}(t-t_0) \right] + \lambda' \sinh \left[ \frac{\kappa}{2}(t-t_0) \right] \right\} \\ 725 &= \frac{F_c}{C_u} e^{(\hat{\lambda}/2)(t-t_0)} \left\{ \frac{\hat{\lambda} + 2\gamma'_d}{\kappa} \cosh \left[ \frac{\kappa}{2}(t-t_0) \right] + \sinh \left[ \frac{\kappa}{2}(t-t_0) \right] \right\} \\ 726 \end{aligned}$$

727 I present both results jointly to show the simplicity of the derivatives

$$\begin{aligned} 728 \quad \dot{T}_s &= \frac{F_c}{C_u} e^{(\hat{\lambda}/2)(t-t_0)} \left\{ \cosh \left[ \frac{\kappa}{2}(t-t_0) \right] + \frac{\hat{\lambda} + 2\gamma'_d}{\kappa} \sinh \left[ \frac{\kappa}{2}(t-t_0) \right] \right\} \\ 729 \quad \dot{T}_a &= \frac{F_c}{C_u} e^{(\hat{\lambda}/2)(t-t_0)} \left\{ \frac{\hat{\lambda} + 2\gamma'_d}{\kappa} \cosh \left[ \frac{\kappa}{2}(t-t_0) \right] + \sinh \left[ \frac{\kappa}{2}(t-t_0) \right] \right\} \\ 730 \end{aligned}$$

731 With these derivatives, I can calculate the ratio of the antisymmetric mode derivative to the  
 732 symmetric one that appears in equation (A15)

$$\begin{aligned}
 \frac{\dot{T}_a}{\dot{T}_s} &= \frac{\frac{\hat{\lambda}+2\gamma'_d}{\kappa} \cosh\left[\frac{\kappa}{2}(t-t_0)\right] + \sinh\left[\frac{\kappa}{2}(t-t_0)\right]}{\cosh\left[\frac{\kappa}{2}(t-t_0)\right] + \frac{\hat{\lambda}+2\gamma'_d}{\kappa} \sinh\left[\frac{\kappa}{2}(t-t_0)\right]} \\
 &= \frac{\frac{\hat{\lambda}+2\gamma'_d}{\kappa} + \tanh\left[\frac{\kappa}{2}(t-t_0)\right]}{1 + \frac{\hat{\lambda}+2\gamma'_d}{\kappa} \tanh\left[\frac{\kappa}{2}(t-t_0)\right]}
 \end{aligned}$$

736 Formally, above result have the alternative form

$$\frac{\dot{T}_a}{\dot{T}_s} = \tanh\left[\frac{\kappa}{2}(t-t_0) + \operatorname{arctanh}\left(\frac{\hat{\lambda}+2\gamma'_d}{\kappa}\right)\right]$$

739 This is possible only if  $|(\hat{\lambda}+2\gamma'_d)/\kappa| \leq 1$ . Let us prove that in our case this follows

$$\begin{aligned}
 &\left|\frac{\hat{\lambda}+2\gamma'_d}{\kappa}\right| \leq 1 \\
 &\frac{\hat{\lambda}^2 + 4\gamma'_d\hat{\lambda} + 4\gamma'^2_d}{\hat{\lambda}^2 + 4\gamma'_d\lambda'} \leq 1 \\
 &\hat{\lambda}^2 + 4\gamma'_d\hat{\lambda} + 4\gamma'^2_d \leq \hat{\lambda}^2 + 4\gamma'_d\lambda' \\
 &\hat{\lambda} + \gamma'_d \leq \lambda' \\
 &-\varepsilon\gamma' \leq 0
 \end{aligned}$$

746 the last inequality is always true, since  $\varepsilon, \gamma'$  are positive constants. Thus,

$$\frac{\dot{T}_a}{\dot{T}_s} = \tanh\left[\frac{\kappa}{2}(t-t_0) + \operatorname{arctanh}\left(\frac{\hat{\lambda}+2\gamma'_d}{\kappa}\right)\right] \tag{A21}$$

749 Equation (A21) is an hyperbolic tangent that grows from -1 to 1 in a sigmoidal fashion. It has a  
 750 scaling factor that determines how fast it goes from -1 to 1. It also has a shift that sets where the  
 751 hyperbolic tangent will cross zero. Both the scaling and shift depend on the thermal and radiative  
 752 parameters of the system. Since the shift is negative, after the initial forcing the deep ocean (that  
 753 depends on the antisymmetric mode) warms up slower than the upper ocean. At a latter time, the

754 ratio becomes positive and the contrary happens. The time at which the sign reverses is

$$755 \quad t_1 = t_0 + \frac{2}{\kappa} \operatorname{arctanh} \left| \frac{\hat{\lambda} + 2\gamma'_d}{\kappa} \right|$$

756

### 757 **Variation of the climate feedback parameter**

758 With the solution shown before, the  $NT$ -diagram has a slope

$$759 \quad \frac{\dot{N}}{\dot{T}_u} = \frac{\varepsilon + 1}{2\varepsilon} \left( 1 + \frac{\varepsilon - 1}{\varepsilon + 1} \frac{C_u \kappa}{|\lambda|} \left[ \left( \varepsilon + \frac{C_u}{C_d} \right) \frac{\gamma}{C_u \kappa} - \tanh \left( \frac{\kappa}{2} (t - t_0) + \operatorname{arctanh} \left( \frac{\hat{\lambda} + 2\gamma'_d}{\kappa} \right) \right) \right] \right) \lambda \quad (\text{A22})$$

760

761 The factor is composed of terms that are positive except for the ratio term coming from equation  
 762 (A21). The negative ratio for  $t \in [t_0, t_1)$  clearly generates a more negative slope, whereas for  
 763  $t \in (t_1, \infty)$  makes it less negative. At the start one can get the slope

$$764 \quad \frac{\dot{N}}{\dot{T}_u} = \left( 1 + (\varepsilon - 1) \frac{\gamma}{|\lambda|} \right) \lambda, t = t_0$$

765

766 and at the time of sign reversal

$$767 \quad \frac{\dot{N}}{\dot{T}_u} = \frac{\varepsilon + 1}{2\varepsilon} \left( 1 + \frac{\varepsilon - 1}{\varepsilon + 1} \left( \varepsilon + \frac{C_u}{C_d} \right) \frac{\gamma}{|\lambda|} \right) \lambda, t = t_1$$

768

769 After the sign reversal the factor of  $\lambda$  will only decrease up to

$$770 \quad \lim_{t \rightarrow \infty} \frac{\dot{N}}{\dot{T}_u} = \frac{\varepsilon + 1}{2\varepsilon} \left( 1 + \frac{\varepsilon - 1}{\varepsilon + 1} \frac{C_u \kappa}{|\lambda|} \left[ \left( \varepsilon + \frac{C_u}{C_d} \right) \frac{\gamma}{C_u \kappa} - 1 \right] \right) \lambda$$

771

772 Equation (A22) shows the importance of the ratio of the symmetric and antisymmetric modes. Its  
 773 physical meaning, the relationship between the upper- and deep-ocean warming, sets the strength  
 774 of the variation of the climate feedback, whereas the constant term sets a base enhancement around  
 775 which the feedback evolves. The thermal capacities of the system determine this constant term.

## 776 APPENDIX B

### 777 **Feedbacks and pattern effect in a non-linear planetary budget**

I start with a planetary imbalance considering a variation of the planetary thermal capacity

$$N = (1 - \alpha)S + G - \epsilon\sigma(fT_u)^4 - \dot{C}T_u \quad (\text{B1})$$

where  $S$  is the incoming solar short-wave flux at the TOA,  $\alpha$  is the planetary albedo,  $G$  are the remaining natural and anthropogenic energy fluxes, and the last two terms are the planetary long-wave response and the contribution to the radiative response of a varying thermal capacity. As said in the main text, the ocean circulation and the atmosphere-ocean coupling provide the dynamical component of the thermal capacity.

If I compute the total derivative of  $N$  then

$$\begin{aligned} \dot{N} &= [(1 - \alpha)\dot{S} + \dot{G}] - S\dot{\alpha} - \sigma(fT_u)^4\dot{\epsilon} - 4\epsilon\sigma(fT_u)^3(\dot{f}T_u + f\dot{T}_u) - \dot{C}\dot{T}_u - T_u\ddot{C} \\ &= [(1 - \alpha)\dot{S} + \dot{G}] - \mathcal{R} \end{aligned}$$

Here we can see the first term is the change from a time-evolving forcing. The rest of the terms,  $\mathcal{R}$ , are atmospheric feedbacks or the effects of ocean circulation and ocean-atmosphere interaction. The fourth term contains the Planck feedback. Let us compare all the terms of  $\mathcal{R}$  in comparison to the Planck feedback term  $4\epsilon f\sigma(fT_u)^3\dot{T}_u$

$$\begin{aligned} \mathcal{R} &= S\dot{\alpha} + \sigma(fT_u)^4\dot{\epsilon} + 4\epsilon\sigma(fT_u)^3(\dot{f}T_u + f\dot{T}_u) + \dot{C}\dot{T}_u + T_u\ddot{C} \\ &= 4\epsilon f\sigma(fT_u)^3\dot{T}_u \left[ \frac{S}{4\epsilon f\sigma(fT_u)^3} \frac{\dot{\alpha}}{\dot{T}_u} + \frac{T_u}{4\epsilon} \frac{\dot{\epsilon}}{\dot{T}_u} + \frac{T_u}{f} \frac{\dot{f}}{\dot{T}_u} + 1 + \frac{\dot{C}}{4\epsilon f\sigma(fT_u)^3} + \frac{T_u}{4\epsilon f\sigma(fT_u)^3} \frac{\ddot{C}}{\dot{T}_u} \right] \end{aligned}$$

By inserting former expression of  $\mathcal{R}$  in the total derivative of the planetary imbalance, reordering and dividing by  $\dot{T}_u$ , we get the analogous expression for the slope of the  $NT$ -diagrams

$$\begin{aligned} \frac{\dot{N}}{\dot{T}_u} &= \left[ (1 - \alpha) \frac{\dot{S}}{\dot{T}_u} + \frac{\dot{G}}{\dot{T}_u} \right] \\ &\quad - \left[ 1 + \frac{S}{4\epsilon f\sigma(fT_u)^3} \frac{\dot{\alpha}}{\dot{T}_u} + \frac{T_u}{4\epsilon} \frac{\dot{\epsilon}}{\dot{T}_u} + \frac{T_u}{f} \frac{\dot{f}}{\dot{T}_u} + \frac{\dot{C}}{4\epsilon f\sigma(fT_u)^3} + \frac{T_u}{4\epsilon f\sigma(fT_u)^3} \frac{\ddot{C}}{\dot{T}_u} \right] 4\epsilon f\sigma(fT_u)^3 \end{aligned}$$

The first contribution in the  $\mathcal{R}/\dot{T}_u$  term is 1, representing the Planck feedback. The second contribution is the planetary albedo feedback. It includes the surface albedo feedback as well as

804 the short-wave cloud feedback. The third contribution is the emissivity feedback, to which mainly  
805 contributes the traditional water-vapor feedback. The fourth contribution is a representation of the  
806 lapse-rate feedback. The fifth and sixth contributions are not atmospheric feedbacks but the effect  
807 of the evolving planetary thermal capacity provided by the atmosphere-ocean interaction and the  
808 ocean circulation.

809 Both the fifth and sixth contributions measure the effect of a changing planetary thermal capacity.  
810 The fifth term should be positive but reduces its contribution towards the equilibrium in view of  
811 the modified two-layer model results. In the same context, the sixth contribution should change  
812 sign, in analogy to the linearized model results.

## 813 **References**

814 Andrews, T., J. M. Gregory, M. J. Webb, and K. E. Taylor, 2012: Forcing, feedbacks and climate  
815 sensitivity in CMIP5 coupled atmosphere-ocean climate models. *Geophys. Res. Lett.*, **39** (9),  
816 L09 712, doi:10.1029/2012GL051607.

817 Armour, K. C., C. M. Bitz, and G. H. Roe, 2013: Time-Varying Climate Sensitivity from Regional  
818 Feedbacks. *J. Climate*, **26** (13), 4518–4534, doi:10.1175/JCLI-D-12-00544.1.

819 Ceppi, P., and J. M. Gregory, 2017: Relationship of tropospheric stability to climate sensitivity  
820 and Earth’s observed radiation budget. *Proc. Natl. Acad. Sci. (USA)*, **114** (50), 13 126–13 131,  
821 doi:10.1073/pnas.1714308114.

822 Geoffroy, O., D. Saint-Martin, G. Bellon, A. Voldoire, D. J. L. Olivié, and S. Tytéca, 2013a:  
823 Transient Climate Response in a Two-Layer Energy-Balance Model. Part II: Representation of  
824 the Efficacy of Deep-Ocean Heat Uptake and Validation for CMIP5 AOGCMs. *J. Climate*, **26** (6),  
825 1859–1876, doi:10.1175/JCLI-D-12-00196.1.

- 826 Geoffroy, O., D. Saint-Martin, D. J. L. Olivié, A. Voldoire, G. Bellon, and S. Tytéca, 2013b:  
827 Transient Climate Response in a Two-Layer Energy-Balance Model. Part I: Analytical Solution  
828 and Parameter Calibration Using CMIP5 AOGCM Experiments. *J. Climate*, **26** (6), 1841–1857,  
829 doi:10.1175/JCLI-D-12-00195.1.
- 830 Gregory, J. M., R. J. Stouffer, S. C. B. Raper, P. A. Stott, and N. A. Rayner, 2002: An Ob-  
831 servationally Based Estimate of the Climate Sensitivity. *J. Climate*, **15** (22), 3117–3121, doi:  
832 10.1175/1520-0442(2002)015<3117:AOBEOT>2.0.CO;2.
- 833 Grose, M. R., J. Gregory, R. Colman, and T. Andrews, 2018: What Climate Sensitiv-  
834 ity Index Is Most Useful for Projections? *Geophys. Res. Lett.*, **45** (3), 1559–1566, doi:  
835 10.1002/2017GL075742.
- 836 Hawkins, E., and R. Sutton, 2009: The Potential to Narrow Uncertainty in Regional Climate  
837 Predictions. *Bull. Amer. Meteor. Soc.*, **90** (8), 1095–1107, doi:10.1175/2009BAMS2607.1.
- 838 Jiménez-de-la-Cuesta, D., and T. Mauritsen, 2019: Emergent constraints on Earth’s transient and  
839 equilibrium response to doubled CO<sub>2</sub> from post-1970s warming. *Nat. Geosci.*, **12** (11), 902–905,  
840 doi:10.1038/s41561-019-0463-y.
- 841 Kiehl, J., 2007: Twentieth century climate model response and climate sensitivity. *Geophys. Res.*  
842 *Lett.*, **34** (22), L22 710, doi:10.1029/2007GL031383.
- 843 Mauritsen, T., 2016: Clouds cooled the Earth. *Nat. Geosci.*, **9** (12), 865–867, doi:10.1038/  
844 ngeo2838.
- 845 Meraner, K., T. Mauritsen, and A. Voigt, 2013: Robust increase in equilibrium climate sensitivity  
846 under global warming. *Geophys. Res. Lett.*, **40** (2), 5944–5948, doi:10.1002/2013GL058118.

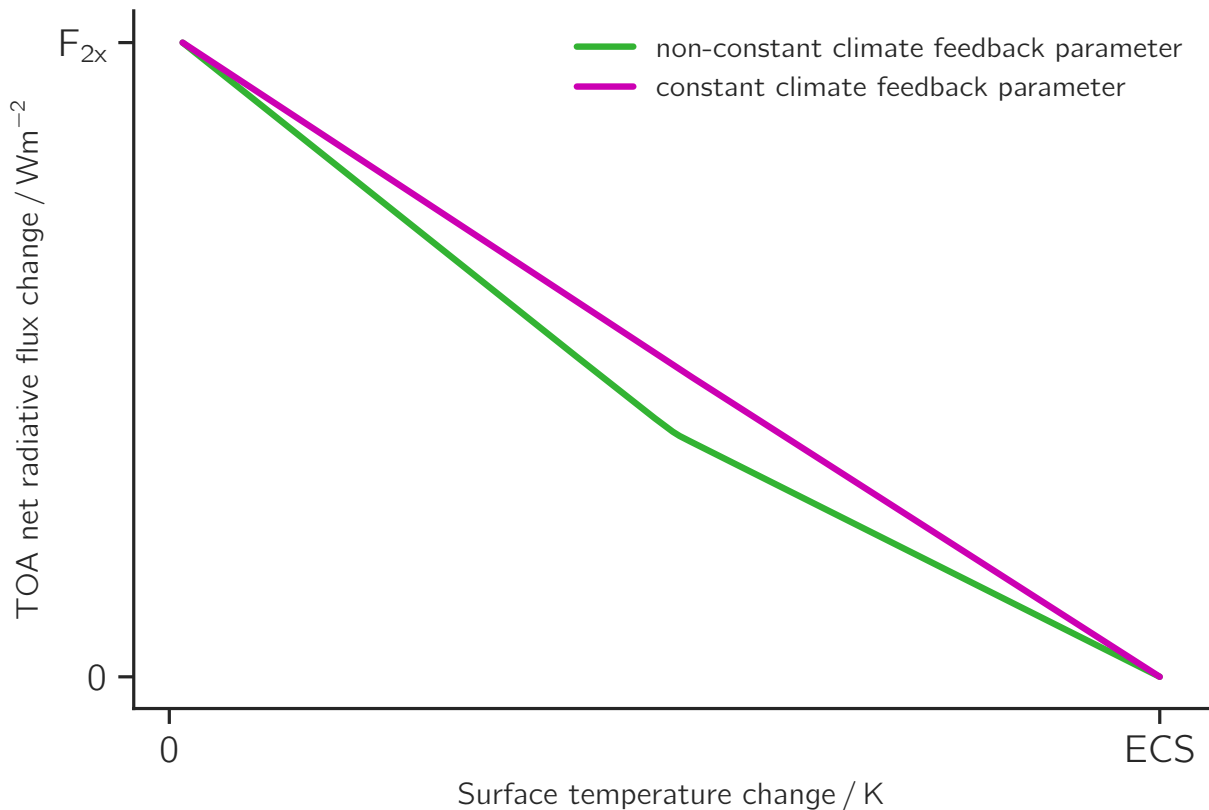
- 847 Rohrschneider, T., B. Stevens, and T. Mauritsen, 2019: On simple representations of the  
848 climate response to external radiative forcing. *Climate Dyn.*, **3 (5-6)**, 3131–3145, doi:  
849 10.1007/s00382-019-04686-4.
- 850 Senior, C. A., and J. F. B. Mitchell, 2000: The time-dependence of climate sensitivity. *Geophys.*  
851 *Res. Lett.*, **27 (17)**, 2685–2688, doi:10.1029/2000GL011373.
- 852 Stevens, B., S. C. Sherwood, S. Bony, and M. J. Webb, 2016: Prospects for narrowing  
853 bounds on Earth’s equilibrium climate sensitivity. *Earths Future*, **4 (11)**, 512–522, doi:  
854 10.1002/2016EF000376.
- 855 Winton, M., K. Takahashi, and I. M. Held, 2010: Importance of Ocean Heat Uptake Efficacy to  
856 Transient Climate Change. *J. Climate*, **23 (9)**, 2333–2344, doi:10.1175/2009JCLI3139.1.
- 857 Zhou, C., M. D. Zelinka, and S. A. Klein, 2016: Impact of decadal cloud variations on the Earth’s  
858 energy budget. *Nat. Geosci.*, **9 (12)**, 871–874, doi:10.1038/ngeo2828.

859 **LIST OF FIGURES**

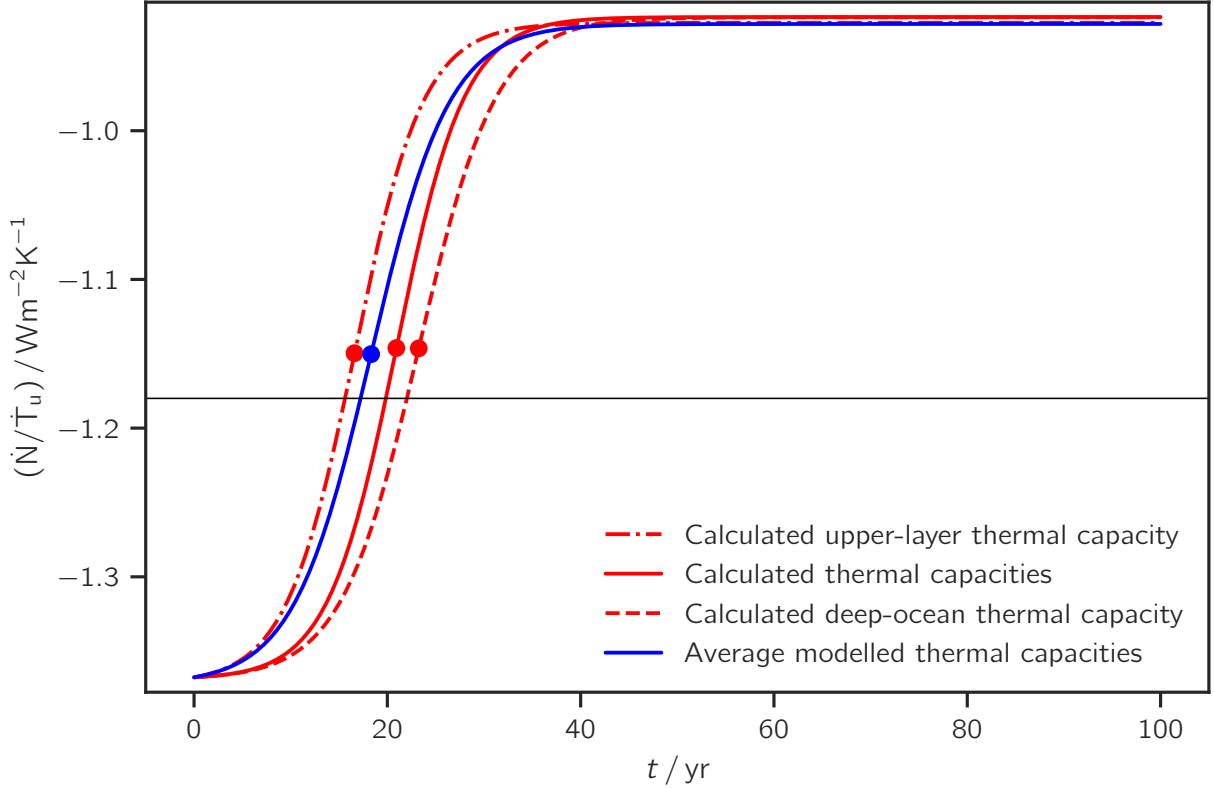
860 **Fig. 1.** Schematic representation of an  $NT$ -diagram for constant forcing due to a doubling of the  
861 atmospheric carbon dioxide concentration ( $F_{2x}$ ). Magenta line represents the relationship  
862 between the TOA net radiative flux change with the surface temperature change if the  
863 feedback mechanisms on surface warming were constant (constant slope). Green line shows  
864 the case found in most models, where the slope varies throughout the process. Given that most  
865 models are not run until equilibrium, the evolving slope introduces considerable uncertainty  
866 in the equilibrium climate sensitivity (ECS) estimates . . . . . 42

867 **Fig. 2.** Evolution of the slope of an  $NT$ -diagram. Blue solid line, with the average parameters  
868 from CMIP5 models obtained by Geoffroy et al. (2013a). Red solid line, with the thermal  
869 capacities as calculated by Jiménez-de-la-Cuesta and Mauritsen (2019). Red dashed line,  
870 with  $C_d$  as in Jiménez-de-la-Cuesta and Mauritsen (2019). Red dash-dotted line, with  $C_u$  as  
871 in Jiménez-de-la-Cuesta and Mauritsen (2019). Dots represent the slope values when the  
872 ratio term  $\dot{T}_a/\dot{T}_s$  has the sign reversal. Thin black line is the constant  $\lambda = -1.18 \text{ W m}^{-2} \text{ K}^{-1}$ . . . . 43

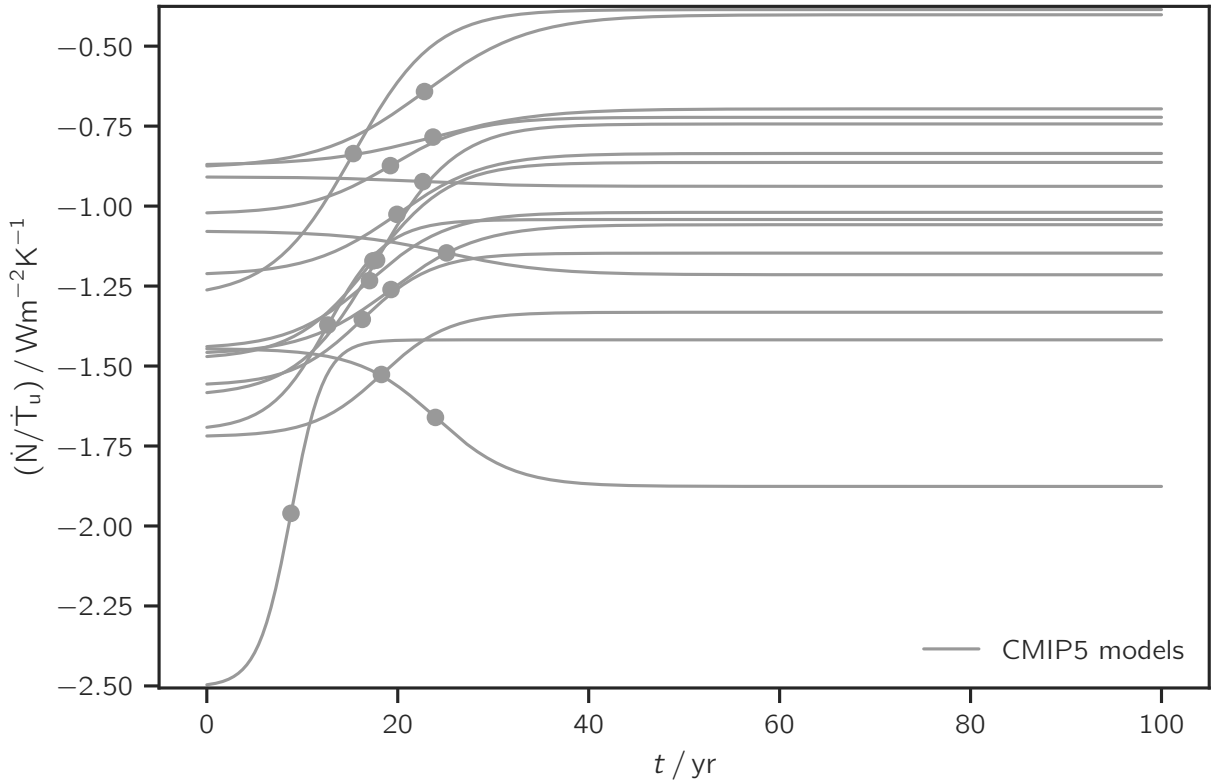
873 **Fig. 3.** Evolution of the slope of the  $NT$ -diagram. CMIP5 model behaviour using the fitted pa-  
874 rameters presented by Geoffroy et al. (2013a). Dots indicate the time of the sign reversal.  
875 Note that three models (CNRM-CM5.1, BNU-ESM and INM-CM4) show a steepening slope  
876 instead of flattening. For these models, the fitted  $\varepsilon$  is lesser than one. . . . . 44



877 FIG. 1. Schematic representation of an *NT*-diagram for constant forcing due to a doubling of the atmospheric  
 878 carbon dioxide concentration ( $F_{2x}$ ). Magenta line represents the relationship between the TOA net radiative  
 879 flux change with the surface temperature change if the feedback mechanisms on surface warming were constant  
 880 (constant slope). Green line shows the case found in most models, where the slope varies throughout the process.  
 881 Given that most models are not run until equilibrium, the evolving slope introduces considerable uncertainty in  
 882 the equilibrium climate sensitivity (ECS) estimates



883 FIG. 2. Evolution of the slope of an  $NT$ -diagram. Blue solid line, with the average parameters from CMIP5  
 884 models obtained by Geoffroy et al. (2013a). Red solid line, with the thermal capacities as calculated by Jiménez-  
 885 de-la-Cuesta and Mauritsen (2019). Red dashed line, with  $C_d$  as in Jiménez-de-la-Cuesta and Mauritsen (2019).  
 886 Red dash-dotted line, with  $C_u$  as in Jiménez-de-la-Cuesta and Mauritsen (2019). Dots represent the slope values  
 887 when the ratio term  $\dot{T}_a/\dot{T}_s$  has the sign reversal. Thin black line is the constant  $\lambda = -1.18 \text{ W m}^{-2} \text{ K}^{-1}$ .



888 FIG. 3. Evolution of the slope of the  $NT$ -diagram. CMIP5 model behaviour using the fitted parameters  
 889 presented by Geoffroy et al. (2013a). Dots indicate the time of the sign reversal. Note that three models (CNRM-  
 890 CM5.1, BNU-ESM and INM-CM4) show a steepening slope instead of flattening. For these models, the fitted  $\varepsilon$   
 891 is lesser than one.